Antibacterial and Anticancer Drugs - Interaction with DNA

(i) Antibacterial Fluoroquinolones

(ii) Anticancer *cis*-Platinum(II) Complexes

A Thesis

Submitted for the Degree of

Philosophiæ Doctor

by

Tormod Skauge

Department of Chemistry
Faculty of Sciences
University of Bergen
2006

Preface

This thesis submitted for the degree of *Philosophiæ Doctor* (Ph.D) at the University of Bergen consists of a summary and 4 papers. One of the papers is published, one paper submitted to Journal of Inorganic Biochemistry and two papers are about to be submitted. All of the work has been carried out during the period 2001-2005, at The Department of Chemistry, University of Bergen under the supervision of Prof. Dr. Einar Sletten and at Laboratoire de Chimie et Biochimie Pharmacologiques et Toxicologiques, Université René Descartes, Paris, France, under the supervision of Dr. Jiří Kozelka. Prof. Dr. Einar Sletten is the principal supervisor for this thesis, while Dr. Jiří Kozelka joined as a co-supervisor in 2002. This work has been financed through a PhD stipend from the Norwegian Research Council (NFR).

The living standard and life expectancy has increased dramatically over the last century. It is clear that neither had been possible if not for the exponential growth in discovery and, equally important, application of new drugs to combat deceases. The benefits of this development have been unequally distributed in the world and in the battle for equal opportunities, the advances of the free academic scientific community are vital. Publication of free, basic science is the best way of preventing privatisation of knowledge, especially on drugs and drug mechanisms. Ideally, public knowledge will give the developing countries the possibility to produce drugs at lower costs, as cost is the major hindrance for application of drugs in poor countries. However, drug development is a complicated issue. The development costs are astronomical, between $ 500 million and $ 2000 million per drug, and the estimated development time is about 10 years. When typically only 1 in 1000 drugs are successful, it is clear that the turnover has to be high. This is true e.g. for a drug like ciprofloxacin (studied in this thesis) which brings in more than $ 1000 million annually. Patenting prevents the development of similar drugs and it is the hope that the publication of free, basic science can limit the patents applied. This would give the developing countries a possibility to offer alternatives to the expensive drugs offered from the industrialized countries and thus improve health for a majority of the world's inhabitants. It is the hope that this thesis can contribute to the understanding of the complex interplay

between DNA as intracellular target and drugs and enlighten the role of metal ions in these processes.

The subjects covered in this thesis can be classified to relate to interaction between DNA and fluoroquinolone antibacterial agents and between DNA and the anticancer agent cisplatin. The results are discussed in the perspective of elucidating the molecular mechanisms of action of these drugs.

Acknowledgements

The results presented here are the condensate of 4 years of hard work. However, much of the real learning experience has come through experiments which cannot (or should not) be reproduced or are not publishable. It has been difficult to accept that each time I felt I was moving closer to the answer, the new questions arising brought me further away. Looking back, I see that this exploration in circles actually was a spiralling staircase going *up* instead of the way it often felt like, *down*. It is funny how life makes you live the clichés you think you are so aware of.

Many people deserve my sincere gratitude for helping making this thesis possible. Firstly, I would like to thank my supervisor over 7 years, Prof. Dr. Einar Sletten. Einar's belief in me has been a great encouragement and made me set out on many new paths seeking answers. Often these paths ended in a complete fog, but Einar's remarkable ability to see the essence of the problems was the compass leading the way out. Einar has an astonishing memory and in discussions often comes up with detailed information from articles or conferences from decades ago. His broad knowledge makes discussions with him tough, but enlightening. Not to forget his great sense of humour which has made the time in his lab a thoroughly enjoyable one. The only negative thing I can say about Einar is that he should be polite enough to slow down when cross-country skiing with younger people.

Dr. Jiří Kozelka is one of the foremost experts in Europe on molecular dynamics simulations of metal-DNA systems and it was an honour to be accepted to his lab. Jirka is not only a great intellectual, but quickly turned into a good friend through his youthful mindset. I am very grateful for the kindness he showed in making the stay in Paris socially very enjoyable, bureaucratically easy and intellectually challenging. The race for unravelling the secrets of the self-cleaving ribozyme was a very exiting time. In this connection I would also like to thank Dr. Eric Guittet and Dr. Jean-Louis Leroy at the national NMR centre at CNRS in Gif-sur-Yvette for allowing me to be a guest in their labs. I learned a lot from these weeks. Thanks also to my colleagues in Paris, especially Dr. Sophie Bombard, Dr. Olivier Delalande, Kateřina Chválová and Sandrine Perrier (for the baby pram!). Both in Paris and in Bergen it has been a great pleasure, both personally and professionally, to work with Dr. Stéphane Teletchéa. He is a wizard in computer science and a tough opponent in biochemical discussions. I am very grateful for the extraordinary effort he made in teaching me all the practicalities of MD simulations and administration of linux clusters, making it possible to establishing MD as a technique at the Department of Chemistry in Bergen.

Dr. Iztok Turel introduced our group to the fluoroquinolone field and has been deeply involved in the studies undertaken. His relentless work to put together an international group to work on fluoroquinolones has been a great inspiration. The use of different techniques made our collaboration particularly exciting. It was a pity that the opportunity never came to visit his lab and share some of the wonderful Slovenian wines. Many thanks also to Dr. Nataša Ulrih and Dr. Petra Drevenšek for stimulating discussions.

Thanks to my colleagues at the Department of Chemistry, the time there was a great time in my life. Especially, I want to thank Dr. Jo Vinje with whom I shared office the last 5 years. While people have come and gone in the NMR group, Jo has always been there, ready to help with everything from recording spectra to carrying the washing machine out of my flat. It has been great to share office with you Jo and I will miss it in the future. Thank you also Magnus (for coffee breaks and ofloxacin discussions), Erlend (for introducing me to linux), Yangzhong, Leonardo (for Panetone), Britt Elin, Bjørn, Trond Ivar and Phillipp (for proof reading). The NMR group has been very helpful and especially Atle Aaberg has been an invaluable help whenever there were problems with the 400 MHz (almost daily) or with the new 600 or 500 MHz (since they arrived) instruments. Even though it was a frustrating time. Atle was always willing to help no matter when you asked and he even had a complementary smile. Takk Atle !

I should also mention the anonymous Open Source community that provides excellent, and not to forget *free*, software for academic use. Open source software has been central in the forming of this thesis, both in data analysis, presentation and publication. Particularly the people behind Sparky, VMD, Mandriva, Gimp, Grace and OpenOffice.org deserve my greatest gratitude. Please give them a try !

Finally, I want to thank my friends and my family for support and for helping me to have at least a minimum of a social life outside the department. My greatest gratitude goes to my wife, Martina, and my son, Mathias, who have made great sacrifices, especially during the last two years. My wife has supported me through good and bad days and without her efforts I would never have been able to bring this to a conclusion. I very much look forward to spending more time with them.

Contents

List of papers

I. Petra Drevenšek, Janez Košmrlj, Gerald Giester, **Tormod Skauge**, Einar Sletten, Kristina Sepčić and Iztok Turel.
"X-Ray Crystallographic, NMR and Antimicrobial Activity Studies of Magnesium Complexes of Fluoroquinolones - Racemic Ofloxacin and Its *S*-form, Levofloxacin"
Journal of Inorganic Biochemistry (in print)

II. **Tormod Skauge**, Iztok Turel and Einar Sletten.
"Interaction between Ciprofloxacin and DNA Mediated by Mg^{2+}-ions"
Inorganica Chimica Acta, 2002, 339, 239-247.

III. **Tormod Skauge** and Einar Sletten.
" Antibacterial Fluoroquinolone Agents - Interaction with DNA"
(Manuscript to be submitted)

IV. Stéphane Teletchéa, **Tormod Skauge**, Einar Sletten and Jiří Kozelka.
" Cisplatin Adducts on a GGG Sequence Within a DNA Double-stranded Decamer Studied by NMR Spectroscopy and Molecular Dynamics Simulations"
(Manuscript to be submitted)

Abstract

This thesis is concerned with the interactions of drugs with DNA mediated by metal ions. The interactions of two types of drugs were investigated: fluoroquinolone antibacterial agents, represented by ciprofloxacin (cipro), levofloxacin (levo) and ofloxacin (oflo), and the anticancer drug *cis*-[$Pt(NH_3)_2Cl_2$] (cisplatin). Fluoroquinolones are highly effective antibacterial agents of which some can be administered orally, thereby having major pharmaeconomical advantages over other antibiotics. Cipro and levo are the most widely prescribed fluoroquinolones and are used against a variety of bacterial infections including treatment of infections of the gastrointestinal, respiratory and urinary tracts, selected sexually transmitted diseases and infections in bones, joints, skin and soft tissues. The primary target for fluoroquinolones is DNA and cellular death is caused by irreversible formation of a ternary fluoroquinolone – DNA – DNA Gyrase complex. However, the molecular mechanisms of action are still largely unknown. Does fluoroquinolone bind preferentially to single-stranded (ss) or double-stranded (ds) DNA ? What is the role of the essential divalent magnesium ion ? What is the binding mode for fluoroquinolones to DNA ? This work attempts to improve the knowledge of this interaction by investigating cipro and levo interactions with DNA in the presence and absence of Mg(II) as well as shedding light on the physico-chemical properties of fluoroquinolones. In paper I, hydrothermal complexes of [Mg(*R*-oflo)(*S*-oflo)$(H_2O)_2$]·$2H_2O$ and [Mg(*S*-oflo)$_2(H_2O)_2$]·$2H_2O$ were synthesized and studied by x-ray crystallography and NMR. In both structures the anionic fluoroquinolone ligands were coordinated through the keto and carboxylate oxygens forming 1:2 Mg:oflo complexes. The two structures were practically identical, except for the orientation of the oxazine methyl group which lead to shorter distance between layers for the Mg(*S*-oflo)$_2$ complex. The complexes showed different solution behaviour both in the preparation of and the solvation of the crystals, indicating that the orientation of the oxacine methyl group plays a significant role for the solution behaviour, e.g. self-associated stacking.

In the first high-resolution study of a fluoroquinolone-DNA interaction (paper II), the influence of divalent Mg-ions on the ciprofloxacin affinity for ds-DNA and subsequent implications for the binding mode were investigated. The results showed that ciprofloxacin binds to DNA in both the presence and absence of Mg(II)-ions. In the absence of Mg(II), both major and minor groove binding were observed, while in the presence of Mg(II), the

preferred binding site was the minor groove as evident from several cipro-DNA NOE cross-peaks.

The Mg(II)-mediated interaction of levofloxacin with two different ds-DNAs was investigated in paper III. Contrary to the observations for ciprofloxacin, levo did not bind to either of the oligomers in the absence of Mg(II). However, in the presence of physiological concentration of Mg(II), levo was found to bind to both oligomers as evident from several NOE cross-peaks. Non-specific binding to both the major and minor groove and interaction with the terminal base pair was observed for both oligomers. Restrained molecular dynamics simulation showed that the minor groove conformation was particularly favourable due to the perfect fit of levo in the minor groove, in accord with the molecular docking results for ciprofloxacin (paper II). One of the oligomers showed levo intercalation between a central GpG step at higher ratios of levo to DNA.

The last part of the thesis is concerned with the interaction of the antitumor agent cisplatin with DNA. Cisplatin is the world's most used metal-based anticancer drug and has been in clinical use since 1978. For the first time a structural characterisation of a cisplatin adduct to a ds-DNA containing a GGG sequence has been undertaken. The cisplatin-DNA adduct was investigated using NMR and molecular modelling. The initial G*G*G adduct transformed to a GG*G* adduct through a reversible isomerization reaction. This enabled a comparison of the effects of guanine flanking bases on both the 3´ and the 5´ side of the G*G* cross-link and pyrimidine flanking bases. The results showed that a 3´ flanking guanine has little influence on the G*G* cross-link, while a 5´ flanking guanine induces significant structural perturbations. The context -GG*G*T- was basically similar in structure to the general -pyG*Gpy- context, however the 5´ XpG* step was different in both structure and dynamics. The fact that the isomerization reaction took place suggests that the cisPt - GN7 bond is labile. This would imply that the current models used to describe protein interaction with cisplatin-DNA cross-links should be re-evaluated.

1 Introduction

1.1 Deoxyribose Nucleic Acids - DNA

1.1.1 History

The first discovery of DNA was done by Friedrich Meischer in 1868, but its role in heredity was not recognized before 1944 when Avery and co-workers published their famous result that DNA and not proteins were the carriers of genetic information.[1] The complementary base-pair rule was found by Chargaff in 1950.[2] A milestone in DNA research was the double helix structure which was proposed by Watson and Crick in 1953 based upon X-ray fiber diffraction data.[3] It was immediately obvious how information could pass from one generation to the next by synthesis of DNA complementary strands from parent strands. In 1962 they received the Nobel Prize in Chemistry for the discovery together with Maurice Wilkins.

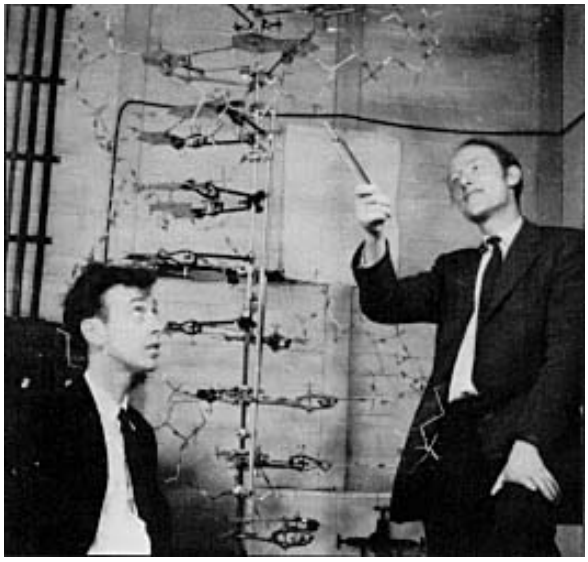

Figure 1.1.1. J.D. Watson and F. Crick with a model of the DNA helix.

However, it was not until the late 1970's that the development of DNA research became explosive, when synthetic DNA fragments became commercially available. The first atomic resolution structure of a single crystal oligonucleotide was published in 1979,[4] the structure of $d(CGCGCG)_2$ with a left-handed structure, known as *Z*-DNA. One year later, the first B-form DNA structure was solved by Dickerson and co-workers.[5] This oligonucleotide, $d(CGCGAATTCGCG)_2$, commonly named the Drew-Dickerson

dodecamer is one of the most studied DNA fragments. During the last 20 years, hundreds of single crystal structures have been solved, providing plenty of detailed information about DNA structure. In later years, NMR has been widely employed to study structures and reactions of DNA in solution. Still, there are many secrets to unlock and keys to find as our hereditary material is being used in ever increasing fields, from traditional medicine and food enhancement to computer chips and biomarkers.

1.1.2 DNA Structure

DNA is a polymer of deoxyribose nucleotides. The polymer is linked by phosphate groups and hydrogen bonds between nucleotides of opposing chains (strands) form a double helical structure. In the cell, the double helix is coiled around histone proteins, creating the nucleosome, which again is supercoiled to form the chromatin that again is supercoiled to higher order structures and finally make up the chromosome. In bacteria, DNA is present in chromosome(s) and in small circular strings called plasmids. The chromosomal organisation of DNA is shown schematically in figure 1.1.2. The superstructure is stabilised by different proteins.

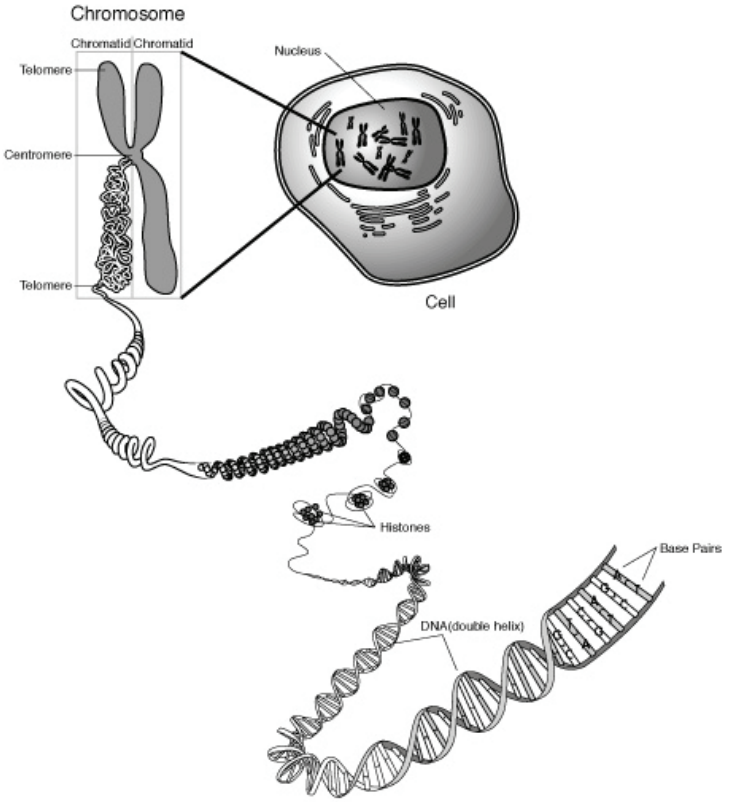

Figure 1.1.2. Simplified view of the DNA organization in the chromosome.

On a molecular level, the double helix consists of only a few components: the deoxyribose sugar ring, the four nucleic bases: adenine (A), guanine (G), thymine (T), cytosine (C) and the phosphate linker. These components, constituting the nucleotide, are seen in figure 1.1.3. In a nucleotide the base is attached via the glycosidic bond to the C1´ carbon of the sugar moiety. The phosphate group is attached to the 5´ and/or the 3´ positions. Due to the asymmetry of the polynucleotide, each DNA strand is directional and read in the 5´ to 3´ direction. The nucleic bases form base pairs (bp) by hydrogen bonding. In Watson-Crick base-pairing, the bases form only two types of pairs: G-C or A-T, according to the Chargaff rules.[2] The result is a double helix, where the two strands are antiparallel and complementary (Figure 1.1.4). Several types of base-pairing are possible, but the Watson-Crick base-pairing is the energetically favoured in B-DNA. The G-C base-pair is stronger than the A-T because of the additional hydrogen bond. This is important when shorter (< 50 bp) DNA fragments, oligomers, are used. In NMR experiments it is common to use 10- to 14 bp oligomers. If the terminal end contains several A-T base-pairs, the terminal base-pairs can separate (so-called fraying) and the double helix can partially unwind.

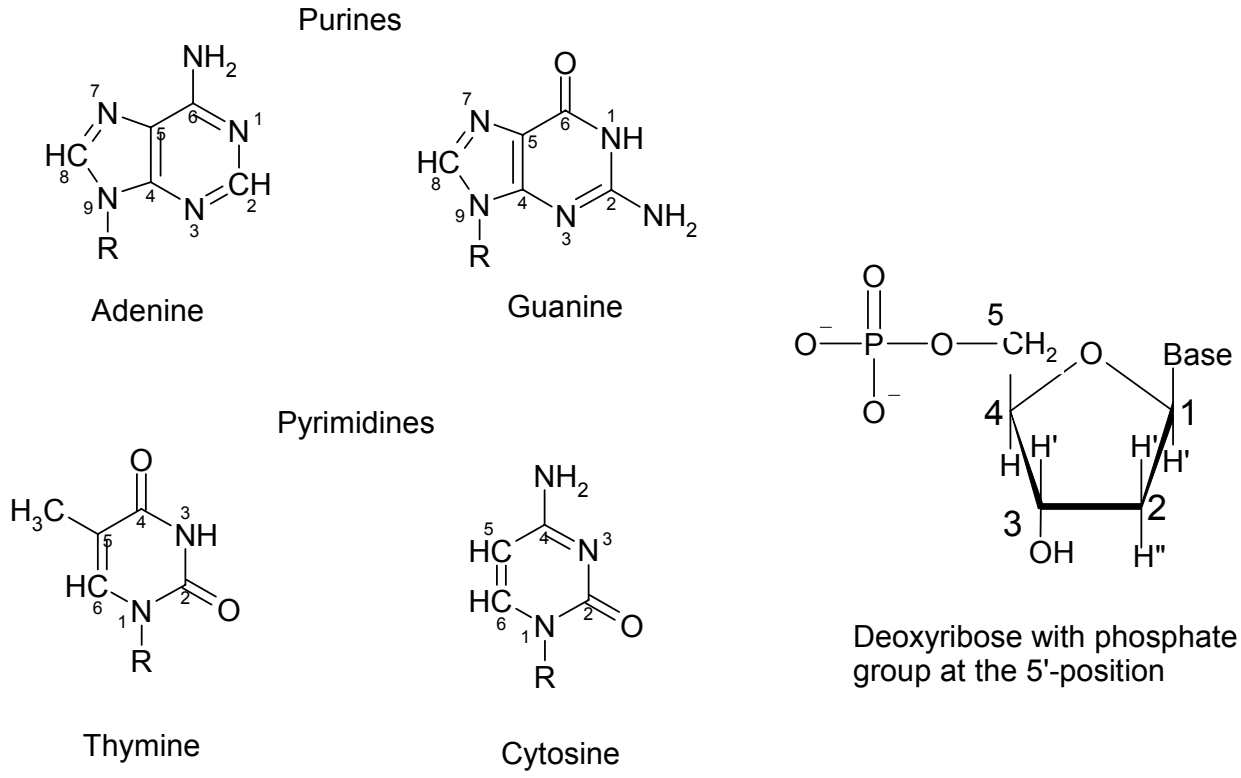

Figure 1.1.3. Schematic drawings of the nucleic bases and of deoxyribose monophosphate.

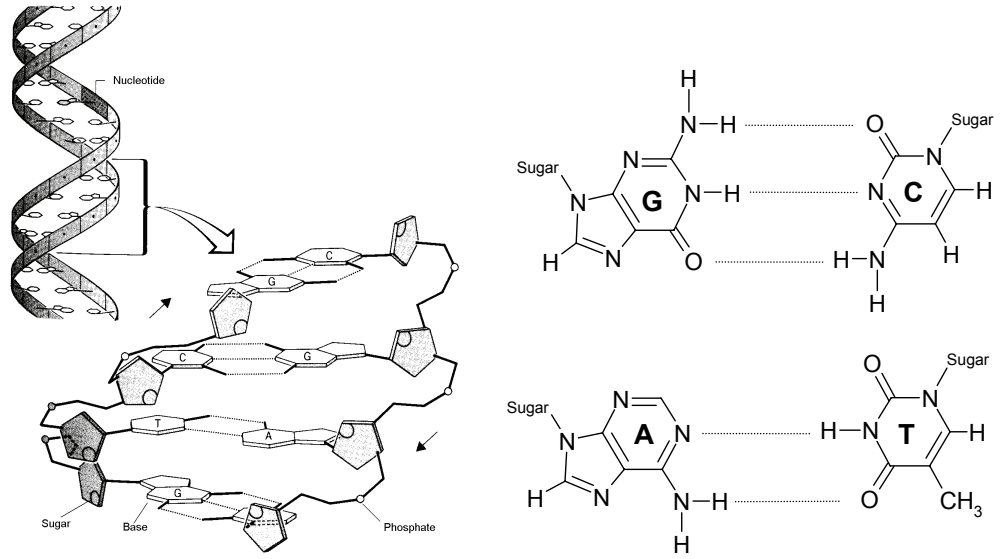

Figure 1.1.4. The DNA double helical structure and complementary base pairing.

The most common conformations of DNA are B-, A- and Z-DNA (Table 1.1.1). B-DNA, which is the most frequently occurring conformation in nature, is a right-handed duplex with 10.4 bp pr helical turn and 3.45 Å distance between the stacked bases. A-DNA is also right-handed, but is wider, having 11 bp pr helical turn. Z-DNA is a left-handed helix with 12 bp pr. helical turn. Transitions between B, A and Z conformations can be induced by e.g. salt concentration and solvent. Also other conformations are known, such as triple helices, three-way and four-way junctions. The human telomere consists of four strands stabilized by potassium ions in the center of the helix.

Table 1.1.1. Structural characteristics for B-, A- and Z-DNA.

Geometry attribute	**A-form**	**B-form**	**Z-form**
Helix sense	right-handed	right-handed	left-handed
Repeating unit	1 bp	1 bp	2 bp
Rotation/bp	33.6°	35.9°	60°/2
Mean bp/turn	10.7	10.4	12
Inclination of bp to axis	+19°	-1.2°	-9°
Rise/bp along axis	2.3 Å	3.4 Å	3.8 Å
Pitch/turn of helix	24.6 Å	35.4 Å	45.6 Å
Mean propeller twist	+18°	+16°	0°
Glycosyl angle	anti	anti	C: anti, G: syn
Sugar pucker	C3´-endo	C2´-endo	C: C2´-endo, G: C2´-exo
Diameter	26 Å	20 Å	18 Å

The backbone of DNA is rather flexible since the phosphate and sugar chain can undergo various kinds of torsions as shown in Figure 1.1.5. The pentose sugar has five torsion angles, $\nu_{0\text{-}4}$. The sugar pucker conformation can be described by two parameters, pseudorotation phase angle (P_s) and amplitude (ϕ_m). Although P_s can take any value, the most commonly observed values are ~162° (C2´-endo, S) and ~18° (C3´-endo, N), illustrated in Figure 1.1.6. The C3´-endo form is commonly found in A-DNA and C2´-endo in B-DNA. These conformations give different values for the coupling constant in sugar protons, NMR spectra may therefore give information about sugar conformations. A geometry change in the DNA helix can lead to changes in sugar conformations; e.g. the bending of DNA induced by the anticancer drug cisplatin is accompanied by a conformation switch from C2´-endo to C3´-endo.[6]

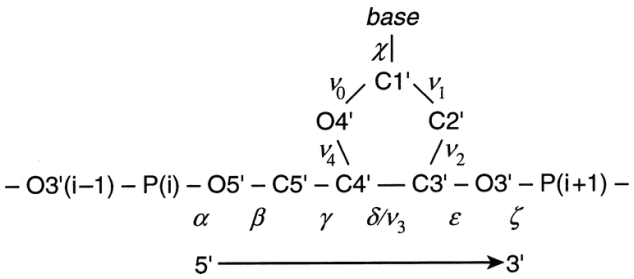

Figure 1.1.5 Torsion angles in the phosphate backbone (α, β, γ, δ, ε, ξ), the glycosidic bond (χ), and the endocyclic torsion angles in the sugar ring ($\nu_0 - \nu_4$).

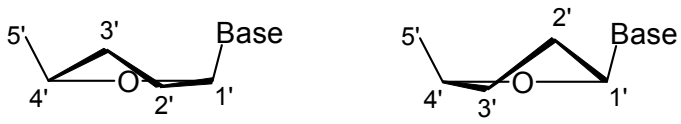

3' - *endo* (N) 2' - *endo* (S)

Figure 1.1.6 The C3´-endo and C2´-endo sugar puckering.

The asymmetry of the strands and the base pairing lead to unequal openings towards the center of the helix. The smaller opening is called the *minor groove* and the larger opening the *major groove*. The major and minor grooves are shown in figure 1.1.7. The sugar-phosphate backbone determines the outer reaction sphere for the DNA. This outer sphere is negatively charged and hydrophilic, while the inner sphere is hydrophobic, resulting in a very high solubility of DNA in water.

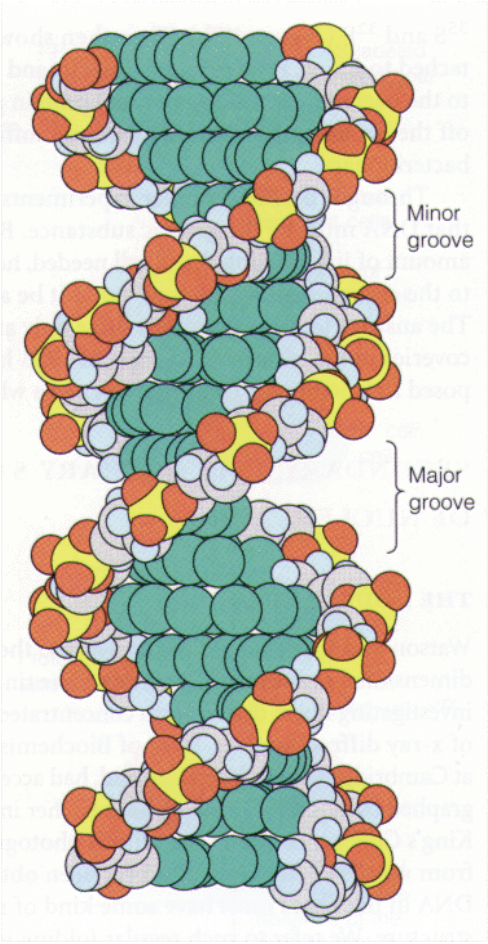

Figure 1.1.7. Schematical drawing of the major and minor grooves of DNA.

Perturbation of base-pair stacking can influence electron distribution in the purine and pyrimidine rings, altering the reactivity of the base nitrogen atoms. Sugiyama and Saito have presented examples concerning electron distributions of HOMOs (Highest Occupied Molecular Orbital) in GG stacking by *ab initio* calculations.[7] Their results showed that the relative orientation of the bases significantly changes the HOMO energy of guanine residues. The induced variation of electron distribution in bases may considerably shift the signals in NMR spectra.

1.1.3 Duplex stability

Four factors are decisive for ordinary B-DNA duplex stability: pH, ionic strength, temperature and solvent. The solvents used in NMR experiments are most often water with 10 % D_2O or 100 % D_2O, which impose no significant differences in stability as compared to pure water. The temperature in NMR experiments can be varied over a wide range, typically 273-313 K. Generally, this is below the melting, or rather dissociation,

temperature, T_m, for most ds-DNA. Both too low and too high ionic strength will lead to duplex instability. The DNA backbone is negatively charged at neutral pH. A layer of counter-ions (typically Na^+, K^+, Mg^{2+} and/or Ca^{2+}) neutralizes the negative charge and stabilizes the structure. If the ionic strength is too low, there will be too few counter-ions and the repulsive forces between the phosphates will give an unstable duplex. Increasing the ionic strength tends to increase the stability of the duplex as more counter-ions neutralize the negative charges of the backbone. However, too high ionic strength will destroy the balance and frequently lead to denaturing of the duplex to single-stranded DNA. At very high ionic strengths like 3-6 M the B-DNA might change conformation to Z-DNA.[8] The pH balance is also important as the base pairs are formed through hydrogen bonds. Too high or too low pH will deprotonate/protonate, respectively, the bases and destabilise the hydrogen bonds. In the minor groove water molecules are interconnected to form the so-called “spine of hydration”. The spine of hydration is also sensitive to protonation states (pH) and ionic strength (ion binding).

1.1.4 Binding modes

There are generally four binding modes for drugs to DNA: minor groove, major groove, surface binding and intercalation.

Minor groove binders are typically long elongated structures with a curvature that fits the curvature of the minor groove. The ligand is fitted between the narrow walls of the groove and stabilized via hydrogen bonds and van der Waals interactions. The minor groove also has a certain flexibility to accommodate for ligands that do not have a perfect fit.

Major groove binders utilize the numerous possibilities for specific hydrogen bonds with donors and acceptors on the nucleic bases providing the basis for both complex stabilization and sequence specificity.[9] Many proteins bind to DNA in the major groove.

Surface binders interact electrostatically and/or via hydrogen bonds to the phosphate backbone on DNA. The binding is often non-specific and is difficult to observe directly. Typically only indirect binding is detectable, for example as a change in the backbone configuration.

Intercalators usually have aromatic ring systems that are inserted into the DNA helix between two neighbouring bases. This leads to increased distance between the bases and local unwinding. Often, the stacking is very little influenced in the rest of the helix. The intercalation is stabilized by stacking interactions, i.e. π-π interactions between the aromatic rings. Also substituents placed in the grooves or on the DNA surface can give additional stabilization of the intercalated structure.[10-12] A typical intercalator is ethidium bromide.

1.1.5 Magnesium binding to DNA.

Magnesium(II) is usually fully hydrated with six water molecules bound in an octahedral conformation when solved in water. According to Chiu and Dickerson,[13] Mg(II) exhibits a sequence-specific binding to DNA in both the major and the minor groove with preference GG > AG > AC. For the GG binding, two hydrogen bonds to O6 and N7 on the 5´-G are donated through water ligands, and a third to the nearby phosphate oxygen. Because the minor groove is much narrower than the major groove, cation binding to the minor groove usually involves interactions between the cation's water ligands and cross-strand base and O4´ atoms of adjacent base-pairs. A fully hydrated cation usually sits at the center of the groove where each of the water ligands can donate maximum two and accept one hydrogen bond to base and backbone atoms. The regular octahedral geometry of magnesium gives an effective ion size of ca. 5.4 Å.

1.2 Antibacterial quinolone mode of action

Quinolones are an important group of antibiotics and several quinolones are in common clinical use (some selected reviews and books[14-17]). The first quinolone, nalidixic acid, was synthesized in 1962 by Lesher et. al.[18] Since then more than 10 000 derivatives have been patented or published.[19] The top three selling drugs, ciprofloxacin, levofloxacin and ofloxacin, each have annual sales of more than one billion dollars. In 2001, letters containing anthrax bacteria were sent to news stations and senators in the USA. The nationwide panic that followed lead to skyrocketing sales of fluoroquinolones, being the preferred drug against anthrax. The fluoroquinolones are popular due to a wide range of activity and possibility of oral administration which saves hospital costs compared to intravenous administration. The drugs act by inhibiting the function of the essential bacterial enzyme DNA Gyrase.

1.2.1 Supercoiling and Topoisomerases

Chromosomal DNA is wound around itself in so-called supercoiling. The supercoiling makes it possible for the 1-2 meter long chromosome to fit within the cell and the supercoiled DNA has an effective diameter of about 1 µm. The winding and unwinding of DNA is accomplished by a class of enzymes called topoisomerases (topo) and supercoiling is achieved by the passage of one DNA strand through another; type I enzymes perform DNA passage after creating a single-strand break, while type II enzymes catalyse the passage of a double-stranded region of DNA through a double-stranded break in the helix. For both classes, the strand passage is accomplished by a transient strand break and resealing step, both mediated by the enzyme. The net level of supercoiling in living bacteria is determined by the balancing activities of topo I and a topo II enzyme called DNA gyrase. The production of topo I and DNA gyrase is self-regulating. An over-activity of one stimulates the transcription of the genes for the other enzyme. Also the transcription of many other genes is very sensitive to the state of supercoiling.[20]

The strand passage is a critical feature common to all topoisomerases as it requires the enzymes to generate breaks in the genetic material. These breaks are stabilized by covalent bonds between the 3´ end (eukaryotic topoisomerase I) or 5´ end (all other) of the newly formed break and the enzyme.[21] Normally, these cleavage complexes are catalytic

intermediates, present only in low concentrations and are therefore tolerated by the cell. However, conditions that significantly increase the physiological concentrations or lifetime of these breaks unleash a myriad of deleterious side effects, including mutations, insertions, deletions and chromosomal aberrations.

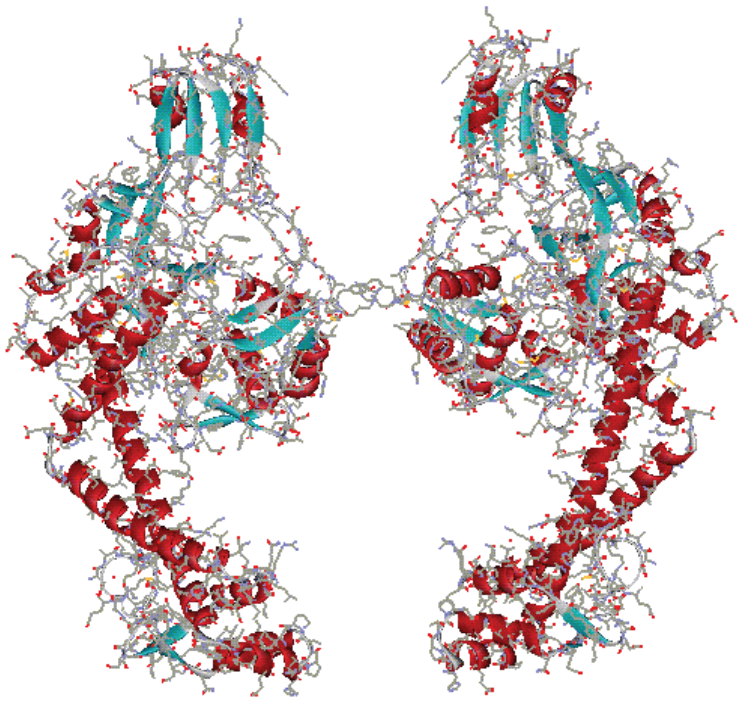

Figure 1.2.1. The active 59kD part of GyrA, containing the DNA cleavage-religation site in the center. The x-ray structure was published by Cabral et al.[22]

It has long been generally accepted that DNA gyrase is the intracellular target for quinolones. DNA gyrase has two subunits, GyrA (97 kDa) and GyrB (90kDa), that are encoded from two different genes, *gyrA* and *gyrB*. The subunits are assembled into a A_2B_2 tetramer.[23, 24] The cleavage-religation site is located at the interface between the two GyrA units (Figure 1.2.1) and the mechanism is explained in Figure 1.2.2. DNA gyrase requires ATP for energy and divalent ions, most readily Mg(II), for strand cleavage and religation.[25, 26]

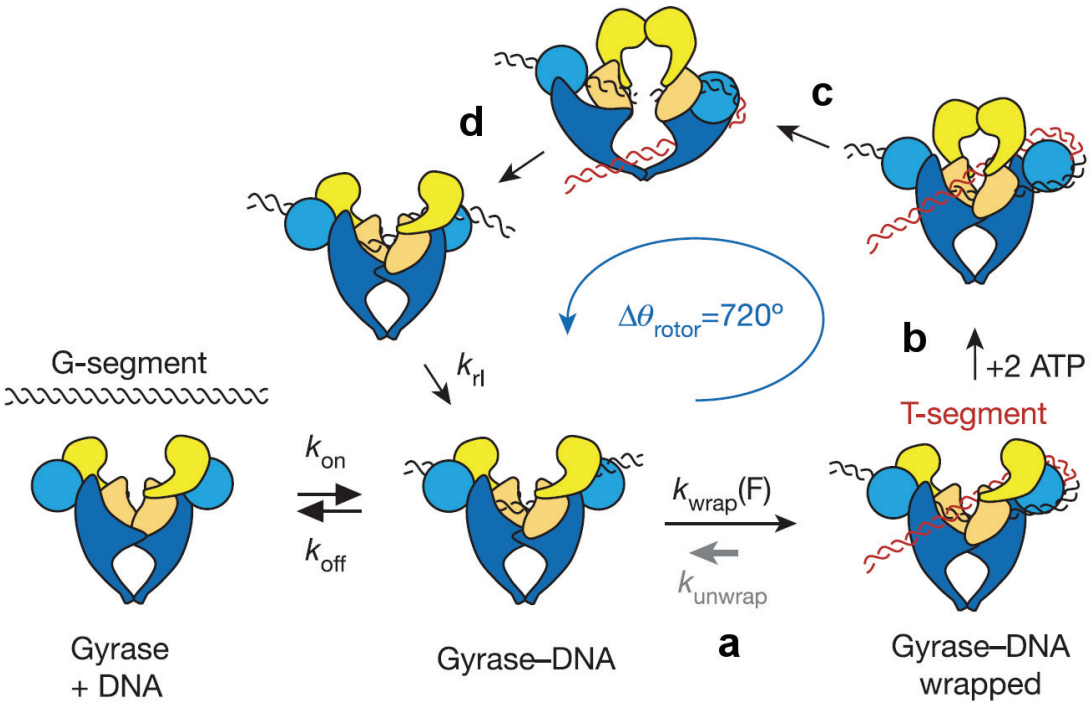

Figure 1.2.2. Proposed DNA cleavage-religation mechanism of DNA Gyrase.[27, 28]
(a) Gyrase binds to a DNA segment as a tetramer and wraps a DNA segment (120 – 140 bp) into a positive supercoil. **(b)** ATP binds to the GyrB subunits and a conformational change occurs. The subunits dimerise, capturing the T-segment. At the same time, a double-strand break is introduced into the G-segment. (the segments are here shown as separate segments to simplify the figure). **(c)** The T-segment is transported through the G-segment break, towards the central hole of the GyrA dimer. **(d)** Following the T-segment passage, the G-segment is religated and the T-segment is released through a transient opening of the primary dimer interface on the GyrA dimer. Religation of the DNA break introduces two negative supercoils on the DNA. ATP hydrolysis promotes enzyme turnover and regenerates the starting state.

The DNA break is formed through a transesterification leading to the attachment of the 5'-phorphoryl group on DNA to the hydroxyl on Tyr-122 on GyrA.[19] The DNA is cut in a sequence-specific manner, creating a 4-bp staggered break on opposite strands of the DNA. Although there is consensus that the cleavage is sequence-specific, there is dispute about the actual sequence. In a study by Morrison et al.[29] the cleavage of four double-stranded DNAs was examined. Each was cleaved between T and G on the one strand, however the cleavage on the complementary strand seemed to have no sequence specificity (Figure 1.2.3).

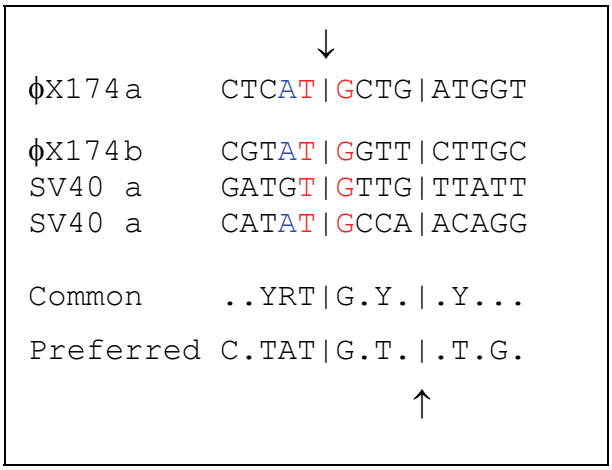

Figure 1.2.3. DNA sequence around gyrase cleavage sites. Only the 14 bp closest to the cleavage site is shown. The bases common to all four sequences are also shown, including purines (R) and pyrimidines (Y). “Preferred” bases are those common to at least three of the four sequences. The arrow on top marks position of gyrase cut on strand shown, arrow at bottom marks position of gyrase cut on complementary strand.

1.2.2 Quinolones history and structure

The quinolone adventure started with the discovery of nalidixic acid (Nal) by Lesher et al.[18] in 1962. As many important discoveries, it was a part-chance discovery. Lesher was investigating by-products from the synthesis of the anti-malarial agent chloroquine, when he discovered that this particular by-product had significant antimicrobial potency. The following decade several new derived structures appeared, increasing the range of Gram negative (G-) bacteria affected by the quinolones. Nalidixic and Oxolinic acid were the leading drugs for almost 20 years, until the breakthrough came in the mid-80’s. Fluorination, primarily at the 6-position, made the quinolones leap from being limited spectrum to be broad-spectrum antibiotics (structures are shown in Figure 1.2.2). The fluoroquinolones had the significant advantage of excellent tissue penetration and low inhibitory concentrations. The most frequent use of fluoroquinolones is treatment of urinary tract infections, bacterial infections of the gastrointestinal tract, selected sexually transmitted diseases and infections of the respiratory tract, in bones, joints, skin and soft tissues. In the '90s, third generation quinolones, like temafloxacin, appeared with lower MICs and even broader spectrum. Unfortunately, this and other succeeding drugs were halted by toxicity, mainly phototoxicity. Many of the third generation drugs have extended ring systems and some have shown promising anti-cancer activity.

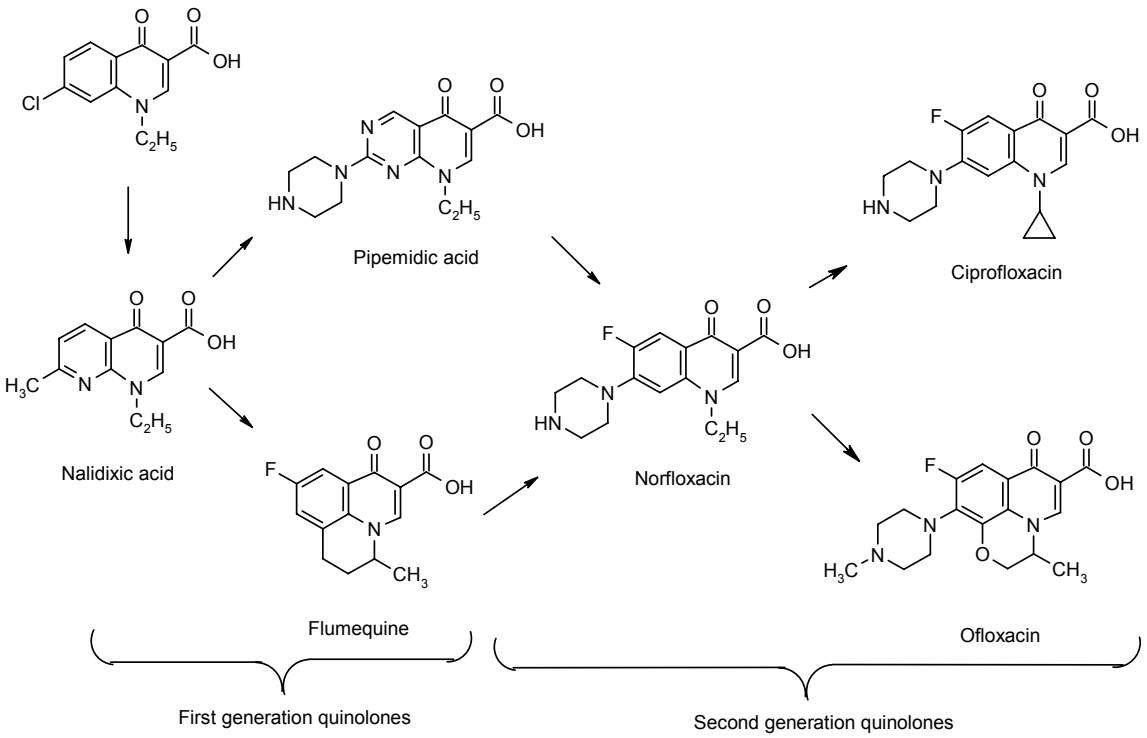

Figure 1.2.2. Some quinolone structures.

The quinolones are rather small compared to many other antibiotics. Many antibiotics have large ring systems that give them an intercalative mode of action or have long chains making them better groove binders. Several structure-activity relationship (SAR) studies have been made to elucidate some of the underlying mechanisms of interaction.[14-17, 30-33] Among the most important findings are: the substituents at position 1 (see Figure 1.2.3) affect the antibacterial spectrum. Rigid, C-8 bridged substituents, as for ofloxacin, improve the activity against Gram positive (G+) bacteria. The substitution of the classical N-alkyl chain for cyclopropyl (ciprofloxacin) leads to a marked increase in the activity against G- bacteria. The positions 2, 3 and 4 are essential and substitution at these positions leads to loss of activity. Metal ions chelate the carboxyl and carbonyl oxygens at positions 3 and 4. The strength of chelation varies with the metal ion: $Al^{3+} > Fe^{3+} > Mg^{2+} > Ca^{2+}$ (decreasing affinity constants).[34] The fluorine at position 6 dramatically increases drug membrane penetration. Position 7 has been exposed with the widest range of substituents. Increased potency and better pharmacokinetics have been observed for cyclic substituents containing secondary or tertiary amino groups. The type of bacteria affected can be fine-

tuned by the substituents on the cyclic rings at this position. Halogen and methoxy substituents at position 8 increase potency, most for halogens which unfortunately also lead to an increase in phototoxicity.

1.2.3 Quinolone Mechanism of Action

The bactericidal effect of quinolones is believed to originate from blocking the function of the essential prokaryotic enzyme DNA Gyrase. DNA Gyrase supercoils in DNA by wrapping the DNA around itself and introduces a transient strand break on both strands. The quinolone binds to the DNA - DNA Gyrase complex and blocks the religation of the cut DNA strands.[21, 35] The ternary complex forms a “roadblock” for the replication machinery. When the replication fork eventually hits the roadblock, the transient double-strand break is converted into permanent double-stranded fragments, no longer held together by protein bridges.[36, 37] The fragments become targets for recombination and repair pathways which in turn stimulate several events, among them: generation of large insertions and deletions and the production of chromosomal aberrations and translocations. When these permanent breaks reach high enough concentrations, events are triggered that ultimately lead to cell death.

The molecular details of the mechanism of quinolone inhibition are still much debated. Although the crystal structure of the active part of the GyrA fragment is published,[22] no high-resolution structure has been published of the ternary DNA Gyrase – fluoroquinolone – DNA complex, or indeed of DNA bound to DNA Gyrase. However, several models have been suggested for the quinolone-Gyrase, quinolone-DNA-DNA Gyrase or quinolone-DNA complexes.

Until the publication by Shen and Pernet[38] in 1985, it was assumed that quinolones bind directly to DNA gyrase. They found that norfloxacin (Nor) bound to DNA and *not* to gyrase. Higher affinity for single-stranded DNA (ss-DNA) than for double-stranded DNA (ds-DNA) and an apparent saturable binding site, inspired a cooperative binding model where pairs of quinolones stack on top of each other. The 2:2 Nor complex is inserted into an opening of the DNA, created at the DNA gyrase binding site. Within this “binding pocket”, the quinolone keto-carboxylate group forms hydrogen bonds to the imino and amino protons of the nucleic bases. The pairs of stacked quinolones are stabilised by hydrophobic interaction of the attached ethyl group. The model has been refined in later years,[39-44] but

remains essentially the same.[17] Later the claim of a saturable binding site was abandoned. A preference for single-stranded poly(dG) > poly(dA) >> poly (dT), poly(dI) and poly(dC) was found from binding assays .[43] However, the binding affinity for poly(rG) and poly(rA) was ~2 times higher than for poly(dG) and poly(dA), respectively, suggesting that RNA could be an intracellular target for quinolones. To our knowledge, this observation has not been followed up in any later publications.

A model involving the presence of Mg(II) ions was proposed by Palumbo and co-workers.[45, 46] The binding of Nor to plasmid DNA was found to be modulated by magnesium concentration. In absence or in excessive amounts of Mg(II), no binding was detected by fluorescence, electrophoretic DNA unwinding or affinity chromatography techniques. In the presence of an intermediate concentration, 1-2 mM, of Mg(II), relatively strong interactions were detected between Nor and DNA. The association constant, K_1, for the Nor-Mg(II) complex was 990 ± 36 M^{-1} at pH 7.0 and showed a slight dependency on salt concentration. Saturation occurred at a Mg(II) concentration of ~10 mM. In the proposed model for the ternary complex, one Mg(II)-ion acts as a bridge between the phosphate groups on the DNA backbone and the carbonyl and carboxyl moieties of Nor. The binding is further stabilised by π-π interactions between the aromatic ring system of Nor and the bases of the nucleic acid. In contrast to the Shen model, Palumbo and co-workers did not find any support for a cooperative binding mode.

Yet another model was proposed by Maxwell and co-workers. Willmott and Maxwell[47] found, using a spin column technique, that radiolabeled Nor bound only to the complex of DNA Gyrase and DNA and not to either of them separately. By replacing the active Tyr-122 for a serine in the GyrA unit, ciprofloxacin bound in similar amounts as to that of the wild-type.[48] Since Tyr-122 is necessary for cleavage of DNA, this indicates that DNA cleavage and single-strand generation are not pre-requisites for quinolone binding to the gyrase-DNA complex as proposed by Shen.[38, 41-43] Kampranis and Maxwell[49] proposed a model where the binding of quinolones to the gyrase-DNA complex induces a conformational change that results in the blocking of supercoiling. The mechanism of action suggested is as follows (see also Figure 1.2.3):

1. Gyrase wraps a segment of DNA around itself. Investigations into the crystal structure of GyrA59,[22] the active region of GyrA, reveal a possibility for a partial unwinding of the DNA in the region around the active Tyr-122.

2. The partial unwinding creates a “DNA bubble” across the active site that “attracts” the quinolone. The quinolone intercalates into the internucleotide space between the bases that flank the site of bond scission. Direct interactions between the bases and the quinolone, and possibly also amino acids of gyrase.
3. The intercalation of the quinolone leads to an even greater deformation of the DNA helix and induces a conformational change in the gyrase-DNA complex. This results in blocking of the strand-passage activity.
4. Furthermore, the conformational change facilitates the covalent bonding between Tyr-122 and the phosphate backbone and the resulting cleavage of the DNA strand.
5. The cleavage of one strand leads to a further unwinding and destabilization of the DNA helix at the active site and promotes the cleavage of the other strand.

Quinolone binding to the gyrase-DNA complex is fast, $k > 10^4\ M^{-1}\ s^{-1}$, while quinolone-induced cleavage is slow: $k_1 = 2.2 \pm 0.5 \cdot 10^{-3}\ s^{-1}$ and $k_2 \approx 4.2 \cdot 10^{-3}\ s^{-1}$ for the first and the second scission, respectively. The fact that the second cleavage is faster than the first, corresponds with the theory that unwinding promotes cleavage. Experiments performed with Ca^{2+} showed that cleavage was much faster with the metal ion present. The Ca^{2+}-ions were suggested to act by shifting the cleavage-religation equilibrium towards the cleaved form. This implies that the cleavage-religation equilibrium is fast in the absence of the drugs and that the complex is predominantly in the ligated form. The altering of conformation due to quinolone binding is thought to disfavour cleavage reaction and drug-induced cleavage is therefore believed to take place only when a favourable base sequence on the DNA is present.

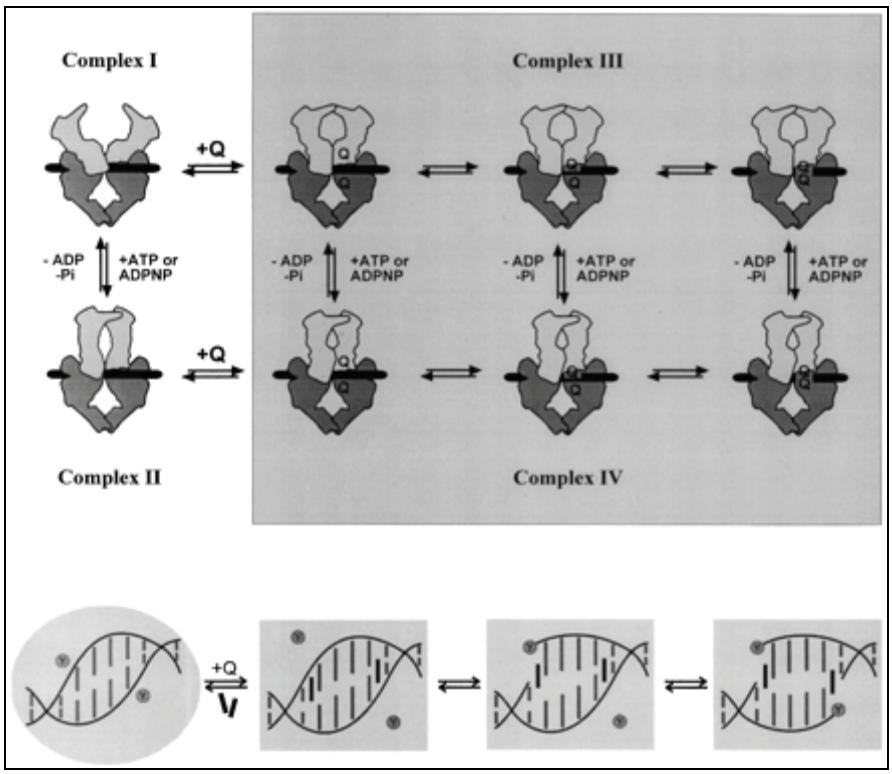

Figure 1.2.3. The Maxwell model for the action of quinolone on DNA gyrase.

In the absence of Mg(II), higher affinity for ss-DNA than for hairpin ds-DNA was found by surface plasmon resonance (SPR).[50] Single-stranded hexamer and double-stranded 16-mer hairpin DNA oligonucleotides were attached to DNA chips and binding of fluoroquinolones was measured. The binding to ss-DNA appeared to be sequence dependent with a preference for TGGCCT (GyrA cleavage site for one DNA investigated) over TAACCT. All interactions were consistent with a fast on-off binding to the chip. The binding was Mg(II)-mediated as both ss-DNA and hairpin ds-DNA exhibited optimal binding at Mg(II) concentrations of 0.5-1.0 mM. The fluoroquinolone concentration was 0.1 mM, i.e. a fluoroquinolone:Mg(II) ratio between 1:5 and 1:10 was required. Binding of ciprofloxacin to ss-DNA in the presence of Mg(II) had a lower K_d-value than softer metal ions, e.g. Cd(II) and Mn(II). This suggested that the softer metal ions bound directly to the nucleic acid bases (N7) with a tighter binding than for Mg(II).

The Kim group suggested two models: a non-classical intercalation model and a non-classical binding in the minor groove. The minor groove model resulted from a non-restrained molecular modelling study taking major and minor groove binding and intercalation into account.[51] Of the binding models investigated the structural features of

the minor groove binding was most in accord with previous fluorescence and CD/LD experiments.[52-55] However, in previous work, a non-classical intercalation model was proposed.[53] LD spectra showed electric dipole transitions corresponding to $\pi \rightarrow \pi^*$ transitions, suggesting a strong π-π interaction with the nucleic acid bases. The angle of Nor with the helical axis (67º-86º) was close to, but not the same as that of a classical intercalator. The orientability of DNA increased with drug concentration, probably due to duplex bending or duplex dissociation near the drug binding site. The interaction was not dependent on Mg(II). Nor was found to bind to both ss- and ds-DNA and the equilibrium constant for interaction with ss-DNA was twice that of ds-DNA. However, the free energy of reaction was the same for both. The reaction for both ss- and ds-DNA was enthalpy driven, as the entropy change was unfavourable (ΔS was negative).

Lecomte and co-workers have studied fluoroquinolone interaction with metals and DNA by ^{19}F NMR. Among their findings is the determination of the binding constant for the pefloxacin-Mg(II) complex, $K_a = 13.0 \pm 0.5 \cdot 10^2\ M^{-1}$.[56] The binding constant increased with drug concentration (range 0.1 – 1.0 mM), probably due to self-associated stacking. The highest degree of self-associated stacking was found at low pH. Pefloxacin was monomeric at concentrations below 0.1 mM, which is 50 times higher than the activity concentration (MIC = 2 μM).[57] Binding to linear DNA was preferred to supercoiled DNA in the presence of Mg(II), suggesting that partial unwinding is not a necessity for quinolone binding to DNA.[58] The ternary complex formation was strongly dependent on the magnesium concentration with an optimum at ~ 2 mM (pefloxacin:DNA:Mg(II) ratio r = 1:40:20), in agreement with the observations by Palú et al.[45]

Tornaletti and Pedrini[59] found a linear increase in unwinding of the DNA in the presence of norfloxacin. At 60 μM Nor, plasmid DNA was unwound one helical turn. The Nor-induced unwinding of DNA was absolutely dependent on Mg(II), later confirmed by Shen et al.[60] and opposed by Son et al.[53]

Several reports have raised the question of sequence-dependent fluoroquinolone binding to ss- and ds-DNA. Bailly et al.[61] found sequence-specificity for poly(dG-dC)•(dG-dC) based on CD/LD experiments. However, while the quinolone binding angle was about 75º

(with respect to the DNA helical axis) for poly(dG-dC)•(dG-dC), it was aligned with the spine of hydration for poly(dAdT)•(dAdT). This has later been confirmed by other groups.[52, 53, 62] Furthermore, substitutions in both major and minor groove interfered with the binding reaction. This strongly suggests that multiple, non-specific binding sites (and possibly modes) are present at the same time, making the experiments difficult to interpretate. The same problem was experienced by Vilfan et al.[62] Ciprofloxacin was found to bind to both ss- and ds-DNA, in a solvent dependent fashion. At low ionic strength (2 mM cacodylic buffer, 1.7 mM NaCl at pH 7.0) cipro showed a 4-fold preference for ss-DNA, while at high ionic strength (10 mM cacodylic buffer, 108.6 mM NaCl at pH 7.0) no preference was found. Melting temperature (T_m) experiments suggested a sequence-specificity for poly-d(AT)•poly-d(AT) over poly-d(GC)•poly-d(GC), however the large difference in T_m for the two sequences, 24.4 ºC and 81.7 ºC, suggests a conservative interpretation of the result. Also Son et al.[54, 63] found that norfloxacin and levofloxacin adopt a different binding mode towards poly[d(A-T)•d(A-T)] as compared to poly[d(G-C)•d(G-C)]. They suggest that the protruding guanine amine group could function as a steric hindrance for fluoroquinolone binding in the minor groove. This is supported by the higher affinity for the minor groove of poly[d(I-C)•d(I-C)] as compared to poly[d(G-C)•d(G-C)].

Sandström et al.[64] investigated norfloxacin interaction with ds-DNA by NMR. Two-dimensional NOESY experiments showed minimal changes in the B-DNA conformation, but selective broadening indicated non-specific groove binding and possible intercalation between CpG steps in the central region of the decamer oligonucleotides.

1.2.4 The role of Magnesium

Magnesium is a prerequisite for DNA Gyrase activity,[25, 26] but high concentrations of the metal decrease the antibacterial effect of quinolones. The binding of Mg(II) to the keto-carboxylic moiety destroys the neutrality of the zwitterionic quinolone. The charged Mg(II)-quinolone complex is less readily taken up into the bloodstream and membrane passage is impaired. This is exemplified by the observation that in urine, where magnesium concentrations can reach 8-10 mM, up to 64-fold increase in the MIC of quinolones was found for some bacteria.[56, 65] The intracellular concentration of Mg(II) in *E.Coli.* is reported to be approximately 100 mM.[66, 67] However, magnesium is predominantly bound,

presumably to ribosomes, and only about 1-2 mM Mg(II) is free in solution in the cell.[68, 69] The bound Mg(II) is readily exchangeable[70] and the low free concentration implies that small changes may regulate the activity of a number of enzymes and thus that Mg(II) plays a regulatory role in the cells. The binding constant for Mg(II) to ciprofloxacin to Mg^{2+} is K_a = 1.30±0.05•10^3 M^{-1},[56] while the binding constant for Mg(II) to DNA is K_a = 22±4•10^3 M^{-1}.[45] The intracellular concentration of quinolone was estimated to be ~0.1 mM[56] and it can be readily assumed that quinolones are complexed with Mg(II) in the bacterial cell.

The above discussion has revealed contradictory information on the role of Mg(II) in the affinity of quinolones to DNA and the DNA – DNA Gyrase complex. Some have reported Mg(II)-mediated binding with an optimal intermediate value[45, 46, 58] while others have reported no such effect.[53]

1.3 Anticancer drug cisplatin and its interaction with DNA

1.3.1 Cisplatin

The cisplatin (*cis*-$[PtCl_2(NH_3)_2]$) adventure started in the 1960's when the Rosenberg laboratory reported inhibitory effect on cell division by this compound.[71, 72] The laboratory was originally investigating the effect of electrical fields on bacterial growth of *Escherichia coli* cells, when they observed a strongly inhibited cell division. Surprisingly, the effect did not come from the induced electrical field, but from a metal complex formed from the reaction of NH_4Cl with the platinum electrodes used in the experiment. The metal complex, cisplatin, rapidly entered clinical trials and was approved for commercial use in 1978. Cisplatin is the most widely used anticancer drug today,[73] and is used against ovarian, cervical, head and neck, esophageal and non-small cell lung cancer.[74-77] Used against testicular cancer it has an astonishing cure rate close to 95 %.[78] However, chemotherapy treatment by cisplatin comes with a price of severe side effects including nausea, vomiting and ear damage as cisplatin not only attacks cancer cells, but also healthy cells. It is therefore important to elucidate the details of the cisplatin mode of action to design new cisplatin analogs that specifically target cancer cells. Furthermore, most cancer cells are insensitive towards cisplatin or develop resistance. There is therefore also a need for cisplatin analogues with a broader range of cytotoxicity. The search for new analogues and the elucidation of the complete mode of action have been going on for more than 40 years and there is an enormous amount of data available for researchers. Still, the picture of how cisplatin works is incomplete.

Cellular DNA has been shown to be the primary target for cisplatin , although cisplatin can react with several other cellular components (membrane phospholipids, RNA, proteins and microfilaments).[79] In the bloodstream, previous to cell membrane passage, the mostly inactive *cis*-$[PtCl_2(NH_3)_2]$ form is protected from reaction by the high salt concentration (> 100 mM). In the cell, the salt concentration is significantly lower (~ 20 mM) and *cis*-$[PtCl_2(NH_3)_2]$ is hydrolysed to the probable active species *cis*-$[PtCl(OH_2)(NH_3)_2]^+$. The hydrolysed product binds to DNA and preferentially to guanine N7 >> adenine N7 > cytosine N3,[80-82] first as a monoadduct, then forming a bidentate adduct. The primary products are

1,2-intrastrand cross-links of GpG (60-65 %) or ApG (20-25 %) sequences.[83, 84] A smaller amount corresponds to 1,3-intrastrand or G N7 – G N7 interstrand adducts.

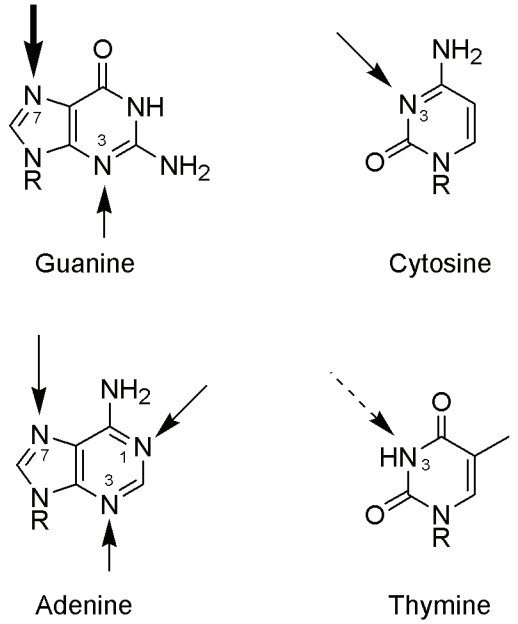

Figure 1.3.1 The most common binding sites on the nucleobases for Pt. The big arrow on guanine indicates the overall favourable coordination site in DNA, the arrow towards thymine is dotted because the proton has to be removed before Pt association.

The formation of these 1,2-intrastrand cross-links alters the duplex conformation. The most dramatic effect is unwinding of the two strands[79] and bending of the DNA double helix (several values for the bend angle are reported in the range 20-80°). The platinated adducts are assumed to be recognized by proteins, followed either by stabilization of the distorted DNA structure or removal of the lesion through repair.[85] The deformation of the DNA structure can interfere with the normal functions of DNA, such as replication and transcription, leading to cellular death by apoptosis or necrosis. The ineffective isomer of cisplatin, transplatin (*trans*-[$PtCl_2(NH_3)_2$]), is not able to form 1,2-intrastrand cross-links. Transplatin forms only 1,3-intrastrand and interstrand cross-links[86, 87] and this might be the reason why transplatin is antitumor inactive.

1.3.2 Sequence selectivity

Cisplatin-DNA sequence selectivity has been given great attention from the research community. Several studies show that cisplatin first binds monofunctionally to guanine N7[88-

[95] and is particularly reactive toward G_n-runs (n ≥ 2). The high nucleophilicity of G_n-runs attracts the positively charged cisplatin monoaqua specie. The lifetime of the monoadduct is relatively long and it has therefore been suggested that the initial monoadduct is crucial for the type of cross-linked adduct formed and thus for the cytotoxic properties of the Pt complex. The main factors influencing the monofunctional binding affinity in DNA are thought to be:

i. Type of bound nucleotide and of the adjacent residues
ii. Steric effects of the Pt complex
iii. Hydrogen binding properties of the Pt-DNA adduct
iv. DNA conformation

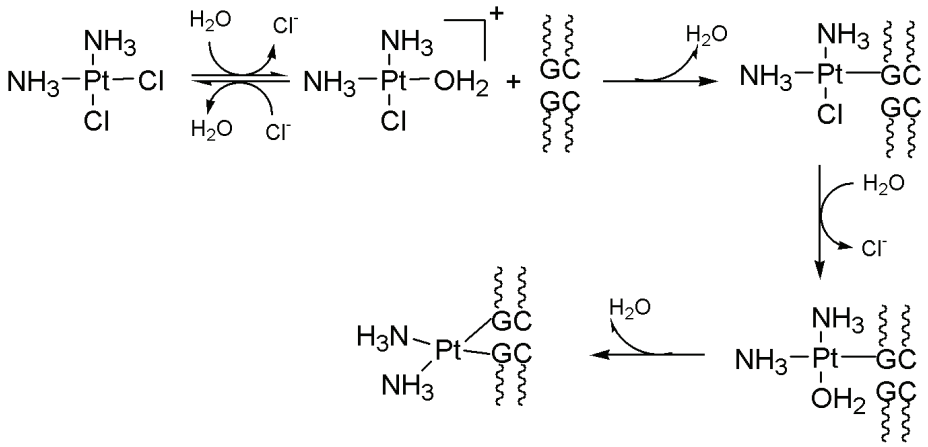

Scheme 1.3.1 Generally assumed mechanism for the formation of cisplatin-DNA adducts.

1.3.3 Sequence specific structural perturbation

The formation of a cisplatin adduct with the GpG bases requires a significant tilting of the bases leading to a perturbation of the regular B-DNA conformation. The structural perturbation has been shown to be specifically recognized by a number of cellular proteins, including proteins with high-mobility group (HMG) binding domains and the TATA box binding protein.[96] It is believed that (some of) these recognition proteins mediate the cellular response which finally induces cell death by apoptosis or necrosis. In some cases, relatively subtle changes in the adduct structure can affect the recognition and the biological effects in a major way. This is exemplified by the cisplatin analogue oxaliplatin which forms similar G*G*-Pt adducts as cisplatin. However, the oxaliplatin-G*G adducts differ in repair efficiency, mutagenesis and translesion synthesis, believed to be related to the differential activity of the two drugs (oxaliplatin is used, in combination with 5-

fluorouracil, for the treatment of colorectal cancers against which cisplatin is inactive). The evaluation of the structural details of the platinum-DNA adducts and of their effects on protein recognition can therefore help to understand why the biological activities of two similar platinum compounds (e.g., cisplatin versus oxaliplatin) are different.

So far only nine cisplatin-DNA adducts have been characterized by NMR and/or x-ray crystallography.[6, 97-104] These structures were extensively reviewed by Ano et al.[105] and found to be basically similar in structure. The cisplatin-GG adduct kinks the double helix approx. ~60 deg towards the major groove and induces N sugar pucker for X of 5´ XG*, 5´ G* and the C complementary to 3´ G*.

The available NMR spectra[97-99, 101, 103, 104] show that platination induces a downfield shift of 0.7 - 1.1 ppm for the 5´ G*-H8 signal, resulting in a chemical shift in the range 8.66 - 8.76 ppm. The 3´ G*-H8 signal is downfield shifted 0.4 - 0.5 ppm, resulting in a shift in the range 8.02 - 8.39 ppm.

The sugar pucker in classical B-DNA is usually regarded to be predominantly S as exemplified in the Arnott B-DNA conformation.[106] A review by Djuranovic and Hartmann[107] on x-ray structures of unperturbed B-DNA sequences shows a relatively high number of N and E sugars; 6.7 % N, 16.1 % E and 77.2 % S. The N/E partition for the individual nucleotides changed significantly when proteins were bound to B-DNA. All the NMR data available for cisplatin adducts of DNA is consistent with a repuckering of the 5´ G* from S to pure N, while the 3´ G* remains S. The sugar of the nucleotide X in the context 5´-XG*G*-3´ has a high degree of N when X = C or T. Sequences with X = G or A have not been investigated. The data for the 5´-CC-3´ sequence complementary to 5´-G*G*-3´ does not show a consistent pattern for the sugar puckers. Puckers S/N, S/S as well as N/S have been found for C(5´ G*) and C(3´ G*), respectively. The reason for the observed variations is not clear, but it seems probable that it is connected to the dynamic motion of the G*C base pairs.

On basis of the NMR data reviewed above, several different models for the adduct have been put forward. The central point of discussion is the stacking *vs* non-stacking of the C bases complementary to the G*G* bases. Other NMR features are well accounted for: a kinked structure bent towards the major groove resulting in a shallow and wide minor

groove; a positive slide and reduced helical twist of the 5′ G*·C base pair; a water-mediated NH_3-phosphate hydrogen bond to either side resulting in repuckering from S to N of the C(5′ G*) sugar; 5′ G* shielding of the 3′ G*-H8, leading to less downfield shift of H8 relative to 5′ G*-H8; a head-to-head (HH) arrangement of the 5′-G*G*-3′ bases with all *anti* χ angles; a positive slide for the 5′ base pair in 5′-(CG*)·(CG)-3′ moving the C-H2′ into the shielding cone of the 5′ G* base. The experimental data for the C(5′ G*)pG step indicates a large separation for the C(5′ G*)-H2′ and G-H8 atoms, but the force fields used in calculations seem to favour a shorter distance, thereby pulling the bases together. Some models also showed large out-of-plane distortions of the 5′ G* N(7)-Pt bond.

1.3.4 Previous studies on platination of a GGG sequence

Marzilli et al. [108-111] investigated the interactions between platinum drugs Ptdien (*cis*-$Pt[Cl_2(en)_2]$, en=ethylenediamine) or cisplatin and the self-complementary DNA oligomer 5′-d(ATGGGTACCCAT)-3′ . Gel electrophoresis experiments using 3′-^{32}P-end-labeling concluded that only 5′-G*G*G-3′ -platination occurred, in contrast to NMR experiments indicating 96% 5′-GG*G*-3′. However, 5′-^{32}P-end-labeling gel electrophoresis gave both adducts. NMR studies suggested that the 5′-GG*G*-3′ adduct exhibited an unusual type of hairpin-like structure. The hairpin structure had a *syn* 3′ G* base and the 5′ G* had an extreme upfield shift. The two bases immediately following the 3′ G* formed a strained hairpin. The concentration of the minor duplex form was found not large enough to be studied. Further studies on the hairpin were performed with the sequence 5′-d(ATGGGTTCCCAT)-3′ where the central –TA- was exchanged for –TT-. This resulted in a more stable hairpin and in addition formation of a small fraction of bulged duplex.[111] The singularity of this hairpin structure did not encourage an extended comparison with the adducts studied in this thesis.

The antitumor activity of cisplatin (*cis*-$[PtCl_2(NH_3)_2]$) has motivated a number of structural studies on adducts with DNA, its likely principal cellular target. The most abundant adduct, the GG intrastrand cross-link, has received particular attention (reviewed by Ano et al.[105] and Elizondo-Riojas and Kozelka[112]). The duplexes contained the context pyG*G*N, (py = pyrimidine; N = T,C, or A) and showed basically similar structures. A duplex oligonucleotide platinated at a GGG sequence has not been studied so far, although G_n sequences (n≥3) are hotspots of platination.[113]

In paper IV we report the first NMR and molecular dynamics simulation study of a 1,2-GG platinum intrastrand cross-link on a sequence containing the context 5´-GGG-3´ and the unprecedented observation of an isomerization of a 5´-G*G*G-3´ to a 5´-GG*G*-3´ duplex adduct.

2 Method

2.1 NMR spectroscopy

The nuclear magnetic resonance (NMR) phenomenon was first discovered in 1946 by the groups of Felix Bloch and Edward Purcell independent of each other. For this discovery, they got the Nobel Prize in Physics in 1952. Since then, NMR spectroscopy has developed to be an indispensable tool for researchers within a variety of fields and especially for chemistry, biochemistry and medicine. The prominent position of NMR is also manifested through the two other Nobel prices given for NMR development: Richard R. Ernst in 1991 for the development of FT (Fourier Transform) NMR and Kurt Wüthrich in 2002 for the development of techniques that make it possible to determine three-dimensional structures of proteins.

The basis for NMR is the existence of nuclear magnetic moment. In a unique chemical environment, the energy level differences of the magnetic moment are also unique. By the use of an external magnetic field, the population of the energy states of the magnetic moments is perturbed. The subsequent relaxation process can be monitored and information about each nuclei and its chemical environment can be extracted. A thorough explanation of the NMR phenomenon is beyond the scope of this thesis and for the interested reader there are numerous sources of information.[114, 115]

Although x-ray crystallography is the prominent technique for structure determination of nucleic acids and proteins, the technique also has several limitations. Some structures do not form crystals and are thus unavailable for x-ray characterization. Likewise, both proteins, nucleic acids and the complexes of drugs can have activity dependent on conformational flexibility and dynamic interchange of states which neither can be represented by crystals. The strength of NMR is thus to provide structures of solution state conformations and give information about conformational dynamics. In some cases also the kinetics of interaction can be followed by NMR. The proton is the by far most frequently studied, but several other nuclei are used routinely, e.g. ^{13}C, ^{15}N, ^{17}O, ^{18}O, ^{19}F and ^{31}P. The accuracy of structure determination by NMR was greatly increased by the application of selective labelling and measurement of dipole-dipole couplings. Through this technique

long-distance (> 5 Å) information can be retrieved. A wide range of experiments ensures that NMR is useful for a broad range of applications. There are however some limitations of NMR that should be pointed out:

1. *Sensitivity.* Compared to many other spectroscopic methods and to biochemical methods like gel electrophoresis, NMR is not very sensitive. Concentrations suitable for NMR are in the mM scale. This often exceeds what is found in biological systems, e.g. the cellular concentrations of cisplatin and ciprofloxacin of animals treated with therapeutic doses are in the μM range. This can be both a phenomenological (different processes can be dominating at higher concentrations) and a practical (economical) problem.

2. *Distance limitation.* Two-dimensional NOESY experiments give high-resolution distance information. However, the NOE detection limit is ~ 5.5 Å which prevents a direct determination of the globular shape of the molecule and of long-distance interactions.

3. *NMR timescale.* The timescale for NMR is typically in the order of milliseconds and several reactions and conformational changes are too fast to be observed by NMR. In this case only the average signal of the species involved in the rapidly exchange is seen.

4. *Symmetry.* Symmetrically arranged groups (or nuclei) give rise to only one set of signals (if they are interrelated by a symmetry operator). This can be a disadvantage in some cases where the symmetry can make it impossible to determine regional interactions. In other cases, e.g. for the self-complementary double-stranded DNA oligomer d(TATGGTACCATA)$_2$ studied in paper III, it was an advantage as the interaction of levofloxacin with the oligomer was detected through the appearance of new signals for the oligomer. The new signals appeared because the binding of the drug broke the C_2 symmetry axis of the oligomer making them unequal.

5. *Overlapping signals.* Nuclei having very similar environment will often overlap, making it hard to assign the exact location within the molecule of that particular nuclei. This is an inherit problem of nucleic acids due to the repetitive pattern of G-C

and A-T base pairs. Due to overlapping signals, NMR structural determination of DNA oligomers is practically limited to lengths of 20 – 40 base pairs without the use of isotope labelling. Another problem is that several interesting DNA signals resonate at frequencies close to that of water. Most samples in this thesis are dissolved in water or D_2O and the concentration of H_2O in these samples is very high compared to the molecule of interest. Therefore, the water signal is suppressed in all the ^1H NMR experiments. Signals close to the water signal are inevitably also suppressed and some are not visible at all.

The NMR spectra were recorded on the following instruments: Bruker DRX-600, (most experiments), DMX-500 and DRX-400. Each instrument was fitted with a pulsed gradient module and a 5 mm inverse probehead. The samples were dissolved in 90/10 % H_2O/D_2O or in 100 % D_2O.

2.2 Molecular dynamics simulations

Due to increasing computational power and cost-efficiency molecular dynamics simulations (MD) has the last years become routinely used in the determination of structures from x-ray crystallography and from NMR experiments. This computational method calculates the time dependent behaviour of a molecular system and allows investigation of the structure, dynamics and thermodynamics of biological molecules and their complexes. By basically using Newton's law of physics and an applied energy function involving a Lennard-Jones electrostatic and a van der Waals term, the velocity vector for each atom is calculated for each time step. In this way, the dynamic behaviour of the molecule is portrayed. The strength of MD simulations is the detailed information it gives on fluctuations and conformational changes. In combination with experimental results, MD has lead to immensely improved interpretations of nucleic acid and protein interactions. A drawback of MD is the demanding calculations involved which means that the timescale is presently at nanosecond level. NMR operates at the millisecond timescale and the gap means that care has to be taken when interpreting results.

Unrestrained dynamics vs restrained dynamics

The traditional MD simulation uses NMR derived distances and torsion angles as restraints for the simulation, usually by applying a harmonic potential with a low-energy central region and exponential energy penalties towards the limiting range. The sequential conformations that result from the calculation at each time step encompass a trajectory. The trajectory is then averaged and the averaged structure energy minimised. If the trajectory was of sufficient length, the trajectory might be searched for sub-structures or "families", i.e. parts of the trajectory where the same structural features are retained throughout the time period. This could be e.g. BI/BII equilibrium for certain base steps that keep recurring in the simulation period. The coordinates of each family are then averaged and each family of structures is compared to each other with regard to physical and chemical relevance, NMR experimental data and overall energy. The "relevant" structures are then compared with the experimental data. In case of discrepancies the experimental data is re-evaluated with regard to structural averaging.

The main disadvantage from doing restrained MD is that the use of experimentally derived restraints *a priori* bias the results. By restricting some distances, a relatively smaller conformational space is explored. In the case of conformational equilibria, this could result in erroneous or incomplete results. If the NMR data indicates a sugar pucker in an N ↔ S equilibrium of 30/70 %, and the restrained dynamics are given input corresponding to this, the averaged MD structure would result in a distorted sugar pucker. The following energy minimalisation would give an S sugar. The detection of substructures would to some degree alleviate this problem by presenting two structures with different sugar puckers. However, this would depend on the MD simulation being sufficiently long and the energetics favourable for S ↔ N transitions to be observed.

In the above example, the use of unrestrained MD could remove the problem as the N ↔ S equilibria would appear without bias. However, the price is paid by the need for running longer and therefore more time-consuming simulations to be able to reproduce the features of the experimental data. Additionally, compared to restrained MD, extra care has to be taken to exclude artefacts arising from non-perfect parameterisation. In restrained MD these artefacts are encountered at a lesser degree as the conformational space is already limited. Unrestrained MD is based on the concept of exploring as much as possible of the conformational space. The quality of the simulation is verified *a posteriori*

by comparing the results with the experimental data. In theory, this will result in a higher degree of observed conformational equilibria and a better assessment of the dynamics.

In paper III only key distances were used in a restrained MD, however the results were evaluated in comparison to the complete set of NMR derived distances. In paper IV, results from an unrestrained 20 ns MD were *a posteriori* compared to the complete set of NMR derived distances. The shorter length of the MD in paper III did not justify running unrestrained MD. The MD protocol used in paper IV is explained below.

MD protocol

The MD simulations were carried out with the SANDER or PMEMD module of the program AMBER Version 6.0[116] implemented on a Beowulf cluster. The parm98[117] force field was extended to account for platinum-guanine coordination, as described by Herman et al.[98] and Elizondo-Riojas et al.[118] The four improper torsion angle terms used to parameterise the bending of the Pt-N7 bonds out of the guanine planes were reduced according to Chval and Šíp[119, 120] in order to account for guanine puckering. The atomic charges and distances for the cis-[Pt(NH3)2(Guo)2]$^{2+}$ moiety were derived from a density functional theory calculation on the 9-methylguanine derivative cis-[Pt(NH3)2(9-Me-Guo)2]$^{2+}$, employing the B3LYP hybrid functional implemented in Gaussian94; the LANL2DZ pseudo-potential/pseudo-orbital basis set was used for Pt and the all-electron basis 3-21G* for the other atoms. The atomic charges were determined from fits to the electrostatic potentials using the Merz-Kollman routine; charges of chemically identical atoms were averaged. The particle-mesh-Ewald method using charge grid spacing of approximately 1 Å with cubic B-spline interpolation and sum tolerance of 10^{-6} Å, was used to calculate the electrostatic energy. A 9 Å cut-off was applied to Lennard-Jones interactions; the non-bonded list was updated every ten steps. The MD simulation employed the SHAKE algorithm (tolerance 0.0005) to all X-H bonds and used a time step of 2 fs. Sixteen counter-ions were placed at the phosphate bisectors approximately 6 Å from the oxygen atoms; no counter-ions were added to the platinated nucleotides. An orthorhombic box of 4853 randomly oriented TIP3P water molecules (64 x 50 x 54 Å) was generated; periodic boundary conditions were applied in all subsequent calculations. The system was first relaxed using four rounds of energy minimization (2 x 500 + 2 x 250 steps) under harmonic constraints limiting the displacements of the solute atoms and counter-ions from their initial positions, with force constants of 100, 50, 25 and 10 kcal/mol

$Å^2$ (1 cal = 4.184 J), respectively. These were followed by 250 steps where a harmonic constraint of 5 kcal/mol $Å^2$ was applied to the solute only, and 500 steps of an unconstrained energy minimization. The system was then heated to 300 K in two rounds of 5 ps with harmonic constraints of 25 kcal/mol $Å^2$ imposed on the solute and counter-ions in NVT conditions. In the first round (0-150 K), the velocities were rescaled, whereas in the second, the system was coupled to a heat bath using the Berendsen algorithm (coupling constant of 0.2 ps). The system was subsequently equilibrated in 13 rounds over 67.5 ps where the constraints were gradually relaxed until a free system was achieved in NPT conditions (1 atm (1 atm = 6.9 kPa); coupling constant 0.2 ps). At three different times a Maxwell distribution of velocities was re-established in order to attenuate the influence of the initial configuration of the system on the dynamics. Finally, a production phase of 25 ns was started. The translational and rotational motions of the solute were removed every 100 steps (0.2 ps). In order to avoid occasional openings of the terminal base-pairs, their W-C hydrogen bonds were reinforced by means of soft distance constraints of 10 kcal/mol $Å^2$. (Analysis of the imino proton resonances has shown that all the base pairs are preponderantly hydrogen-bonded at the temperature of 305 K used for the NMR experiments. Therefore, we did not want to portray the less frequent conformation with opened terminal base-pairs.) The atomic coordinates were stored every 1 ps. The analysis used the programs CURVES for calculation of global helical parameters and the backbone torsion angles, and the CARNAL module of AMBER 6 to determine average structures for different conformational families. The hydrogen atoms of the averaged structures were relaxed using 500 steps of *in vacuo* belly minimization, followed by a full energy minimization with the Generalized Born solvation model implemented in AMBER version 6.0, until a norm of the energy gradient of ≤ 1 was achieved.

2.3 Docking

Docking is a method for locating feasible binding orientations of a ligand molecule on a receptor molecule. The docking program generates numerous orientations of one ligand and ranks them according to one or more scoring functions. Typical evaluation methods include contact score (shape complementarity) and energy score (electrostatic and van der Waals energy). The strength of the docking method is the possibility to screen ligand/receptor interaction prior to performing expensive and time-consuming experiments. In the pharmaceutical industry, docking is applied to screening databases of hundreds of

thousands of pharmacophores in protein/enzyme interactions. Modern computer clusters can perform about 100 000 screenings per day. In this thesis, the docking method was used to supplement the experimental NMR data and aid the interaction analysis.

In docking a representation of the receptor site is first created and subsequently orientations of the ligand are screened against the representation, similar to the creation of a plaster cast of a foot and checking if the shoe fits the plaster. The site of interest on the receptor is selected from a structure file, typically derived from crystallography or NMR. This requires an *a priori* knowledge of the active site. To represent the shape of the interaction site in a simplistic way, the structure model is filled with spheres of a pre-determined size. Where the spheres overlap, a possible interaction site is determined and only these sphere clusters are used for the shape scoring function. To orient a ligand within the site, the sphere of the sphere clusters are "matched" with ligand atoms, making atom-sphere "pairs". The set of atom-sphere pairs is then used to calculate an orientation of the ligand within the site of interest. A translation vector and rotation matrix is then applied where the rmsd of (transformed) ligand atoms and matching sphere centers of the sphere-atom set are calculated and minimized. The sphere generation attempts to capture shape characteristics of the active site with a minimum number of points and without the bias of previously known ligand binding modes.

The electrostatic and van der Waals energies are calculated from the grid function. A fine grid is applied to the structure file and for each grid point the corresponding energies are calculated. The purpose of the grid representation is to make the energy calculations faster. The ligand molecule is then fitted to the grid (not to the receptor molecule itself) and the orientation is a result of an energy minimization of the total ligand-grid energy for the different orientations. Many grid points would be a part of several orientation evaluations, and to save time, the receptor contributions to the score are calculated only once and the appropriate terms are then simply fetched from memory for each evaluation.

In the final step, the orientations from the sphere and the grid calculations are combined and ranked. A grid-based rigid body simplex minimization is used to locate the nearest local energy minimum for each orientation. The best-scoring orientations are then viewed and analysed using a molecular graphics program.

Docking experiments were performed with the DOCK 4.0.1 suite of programs utilizing the Amber parm94 force field. Magnesium was added to the force field assuming no charge dispersion from the metal ion to the keto-carboxyl group. This was judged to be sufficient for main purpose of generating structures aiding the evaluation of the experimental NMR data.

3 Results and discussion

3.1 Antibacterial fluoroquinolones - interaction with DNA oligonucleotides (Papers I - III)

Quinolones are an important group of antibiotics and several quinolones are in common clinical use. Ciprofloxacin (cipro), Levofloxacin (levo) and Ofloxacin (oflo) are the top-selling antibiotics worldwide. Resistance against antibiotics is on the rise and multi-drug resistance will probably become a major problem in the 21st century. It is therefore vital to gather knowledge about the molecular mechanisms of action for antibiotics. The quinolones act by inhibiting the function of the enzyme DNA gyrase, a type II topoisomerase found only in prokaryotic cells. DNA gyrase introduces negative supercoils in DNA[121] by wrapping the DNA around the enzyme. The enzyme then catalyses the breakage of a segment of the wrapped DNA, the passage of another segment of the same DNA through the break and finally the religation of the break.[122] In this way, DNA 'knots' are resolved and the DNA is exposed for replication processes. The enzyme is essential for all bacteria and is therefore an excellent target for antibiotics. Quinolones are assumed to act by blocking the strand ligation and thereby preventing proper replication of DNA, eventually leading to cell death.[35]

A number of models have been suggested to account for the mechanism of action of quinolones (summarised in chapter 1.2). Most of these models require a direct interaction between the drug and either single- or double-stranded DNA.[38, 45, 49, 51] Some have also pointed out the important role of Mg(II) for drug binding.[45, 46, 50, 56, 58] The most prominent theory was put forward by Shen and co-workers[38, 39] where four fluoroquinolone molecules bind in a 2:2 stacked conformation in a bulge in the duplex, created at the enzyme-DNA interaction site. However, most other models are non-cooperative in nature. Additionally, there are discrepancies on the actual binding mode. Several groups have reported conflicting results where CD/LD data has suggested intercalation while fluorescence experiments exclude intercalation and indicate groove binding.[52, 54, 61, 62] An interesting aspect of fluoroquinolone mode of interaction is observed for ofloxacin. Racemic ofloxacin has two enantiomers, *R* and *S*, determined by the conformation of a

methyl group attached to the oxazine ring. The *S*-enantiomer activity against DNA Gyrase is up to two orders of magnitude higher than for the *R*-enantiomer. This is surprising as the methyl group has been regarded as non-functional.[17] Correspondingly, the binding affinity to calf thymus DNA is higher for the *S*-isomer than the *R*-isomer.[40, 63] This suggest a stereospecific interaction with both DNA and DNA Gyrase, which has been a key feature of the Shen model. However, it is difficult to rationalise the stereospecific interaction of *S*-oflo as compared to *R*-oflo, when a number of other fluoroquinolones (e.g. ciprofloxacin, pefloxacin, norfloxacin) with a high diversity of substituents at the R-1 position bind efficiently to DNA and to DNA Gyrase. To solve this and several other key questions on the fluoroquinolone mode of interaction, a high-resolution structure of the DNA-fluoroquinolone-DNA Gyrase complex is much needed. So far only x-ray structures for fluoroquinolone and metal-fluoroquinolone complexes have been solved (recently reviewed by Turel[123]). Furthermore, except for the work presented in this thesis, only one NMR[64] and one molecular modelling study[51] of fluoroquinolone-dsDNA interaction has been published so far.

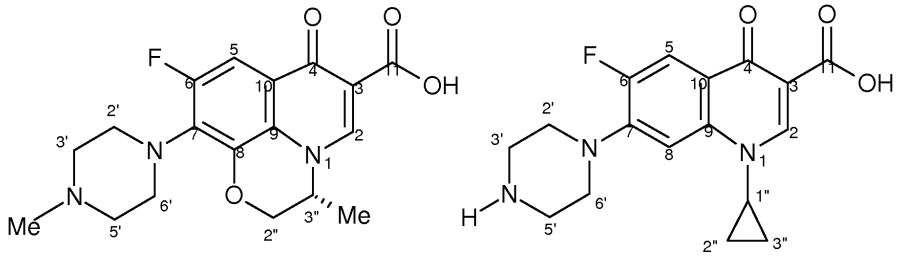

Levofloxacin Ciprofloxacin

Scheme 3.1.1. Schematic drawing of levofloxacin and ciprofloxacin.

In summary, the large amount of work published does not represent a consistent picture of the mode of quinolone-DNA interactions. We have studied the interaction between DNA oligonucleotides and two of the most selling fluoroquinolone drugs: ciprofloxacin and levofloxacin using NMR spectroscopy and molecular modelling. We have focused on the following aspects: (i) the role of Mg^{2+}-ions, (ii) the preference for single- or double-stranded DNA, (iii) binding mode; groove binding and/or intercalation.

Summary of papers

To gain further insight into the role of Mg(II) on fluoroquinolone mode of action, Mg(II) was reacted with racemic ofloxacin. The hydrothermal complexes [Mg(*R*-oflo)(*S*-oflo)$(H_2O)_2]\cdot 2H_2O$ (**O-1**) and [Mg(*S*-oflo)$_2(H_2O)_2]\cdot 2H_2O$ (**O-2**) were synthesized and studied by x-ray crystallography and NMR (**Paper I**). The crystals were isomorphous (monoclinic $P2_1$) and in both structures the anionic fluoroquinolone ligands were coordinated through the keto and carboxylate oxygens forming 1:2 Mg:oflo complexes. The two structures were practically identical, except for the orientation of the oxazine methyl group which lead to shorter distance between layers for **O-2**. The complexes showed different solution behaviour both in the preparation of and the solvation of the crystals, indicating that the orientation of the oxazine methyl group plays a significant role for the solution behaviour, e.g. through self-associated stacking. The solubility of **O-1** and **O-2** was far lower than for the corresponding pure *R,S*-oflo and *S*-oflo drugs. Paramagnetic line broadening measurements with Mn(II) showed that the methylated piperazine nitrogen does not interact with the metal ion. The antimicrobial activity of the complexes against various microorganisms was similar to that of the free *R,S*-ofloxacin and *S*-ofloxacin drugs.

It is known that ATP and Mg(II) are required for the function of DNA Gyrase.[25, 41] Possibly, fluoroquinolones could act by blocking the enzyme-ATP interaction and therefore the interaction of ATP with levo in the presence and absence of Mg(II) was studied by multinuclear NMR (**Paper III**). The results suggested some interaction, however, the binding constant for the ternary ATP-Mg(II)-levo complex appeared to be too low to play a significant role for the inhibitory effect of fluoroquinolones.

The single-stranded DNA sequence 5´-d($C_1C_2T_3A_4A_5T_6C_7C_8$)-3´ was titrated with levo and Mg(II) (**Paper III**). Magnesium chloride was added to stabilize the single-strand conformation. The NMR results showed no significant interaction, which was surprising as ciprofloxacin had been reported to bind preferentially to ss-DNA containing solely TA-base-pairs in the central region.[62] However, the binding preference in the case of ciprofloxacin was observed by fluorescence and CD/LD experiments at lower salt concentrations (< ~5 mM). The higher $MgCl_2$ and NaCl concentrations used in our experiments, 14 mM and 45 mM, respectively, could be one reason for the observed discrepancy.

In the first high-resolution study of fluoroquinolone-DNA interaction (**Paper II**), the influence of divalent Mg-ions on the ciprofloxacin affinity for ds-DNA and its implications for the binding mode was investigated. The results show that ciprofloxacin binds to DNA in both the presence and absence of Mg(II)-ions. In the absence of Mg(II) both major and minor groove binding are observed, while in the presence of Mg(II) the preferred binding site is the minor groove. The minor groove binding was evident from several cipro-DNA cross-peaks, including medium and strong peaks, chemical shift differences and selective line broadening. Docking results suggest, as expected, stabilization by Mg(II) interaction with the phosphate backbone, but also a remarkable complementary fit of the drug in the minor groove (Figure 3.1.1).

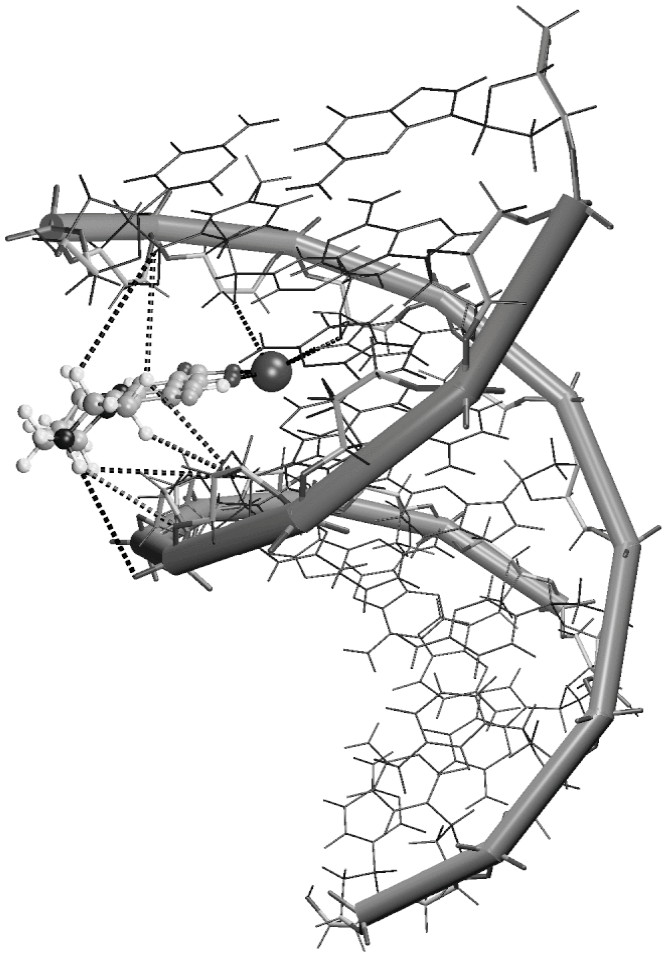

Figure 3.1.1 Docking result showing the Cip-Mg(II) complex anchored in the minor groove of the duplex. Observed NOE contacts and possible electrostatic stabilizing factors are indicated by dotted lines.

The Mg(II)-mediated interaction of levofloxacin with two different ds-DNAs was investigated in **Paper III**. Contrary to the observations for ciprofloxacin, levo did not bind to either of the oligomers in the absence of Mg(II). However, in the presence of physiological concentration of Mg(II), levo was found to bind to both oligomers. This was evident from several medium and weak NOE cross-peaks, as well as line broadening and chemical shift differences. In addition to non-specific binding in the minor groove, interaction with the terminal base pair was observed for both oligomers. For one oligomer, binding in the major groove was also observed. Restrained molecular modelling showed that the minor groove conformation was particularly favourable due to the perfect fit of levo in the minor groove. The minor groove binding was additionally stabilized by electrostatic interaction between Mg(II) and DNA phosphate groups. One of the oligomers showed levo intercalation between a central GpG step at higher ratios of levo to DNA. Selective line broadening of the complementary CpC step suggested that the Watson-Crick base pairing was broken for this step.

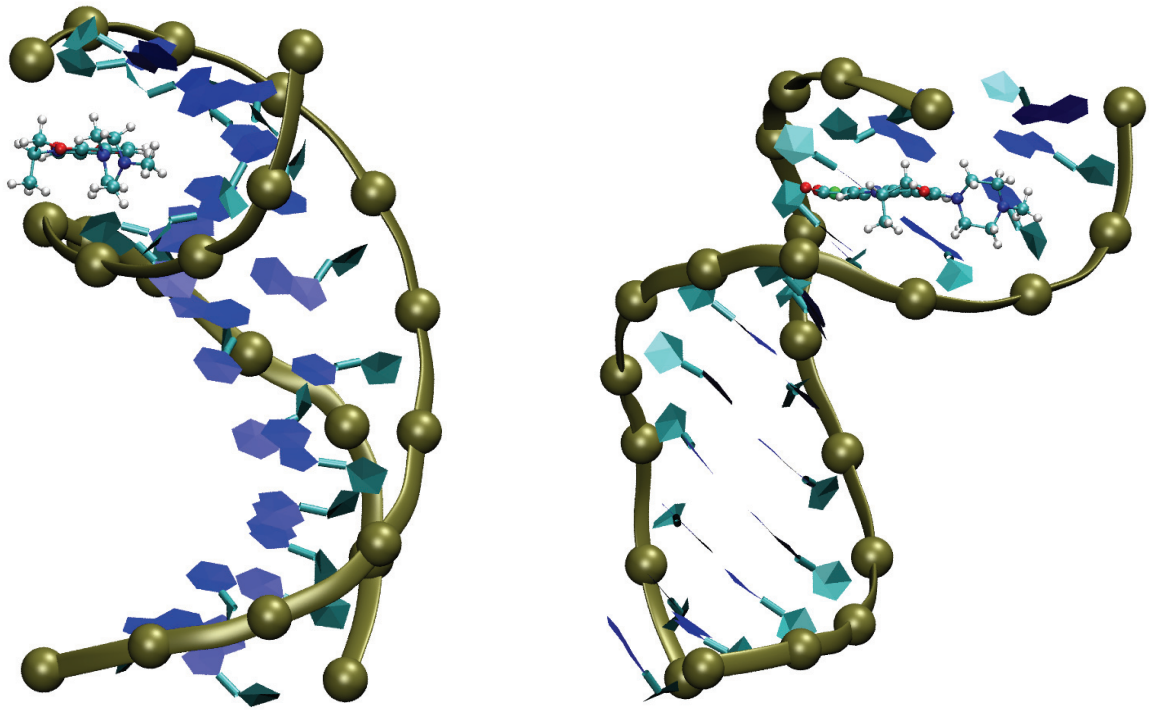

Figure 3.1.2. Levofloxacin-Mg(II) complex bound in the minor groove of the self-complementary sequence 5´-d(TATGGTACCATA). The view is along the minor groove (left) and rotated anti-clockwise 90º (right). DNA bases are blue, sugars cyan, the phosphate backbone is represented by ribbons and the phosphate atoms are exaggerated as gold coloured balls for clarity.

General discussion

The role of magnesium: The physiological concentration of free Mg(II)-ions is 1-2 mM[69], while the intracellular concentration of fluoroquinolone has been calculated to be ~0.1 mM.[56] The binding constant for Mg(II) to ciprofloxacin is $K_a = 1.30 \pm 0.05 \cdot 10^3$ M^{-1}.[56] It can therefore be readily assumed that fluoroquinolones are complexed with Mg(II) in the bacterial cell. This is also consistent with the findings in this thesis, as the selective line broadening of the aromatic fluoroquinolone signals was observed for all the fluoroquinolone-DNA interactions studied. Assuming the Mg(II)-fluoroquinolone complex is the *in vivo* active species, the cooperative model proposed by Shen and co-workers[38, 41] (see Introduction) is unlikely to be entirely correct. The Shen model does not take Mg(II) into account, while several groups have reported a Mg(II)-mediated binding of quinolone to DNA,[45, 46, 58] consistent with our findings in **Papers II** and **III**. A key feature is the possibility for hydrogen bonds between the keto-carboxylic group and DNA bases. Bound Mg(II) would favour interaction with the DNA phosphate groups over direct interaction with the bases. The hydrated Mg(II) ion would also require considerable space in the already crowded interaction site. The 2:2 stacking of quinolones in the DNA "bubble" is proposed to be additionally stabilized by hydrophobic interactions between the two stacks of quinolones. The x-ray structures reported in **Paper I** suggest that an assembly of 4 fluoroquinolone molecules would rather be held together by a stack of 2:1 (fluoroquinolone:Mg(II)) complexes with the hydrophobic part of the fluoroquinolone facing away from the center on each side. The Shen model has been further weakened by the observations that DNA denaturation is not a pre-requisite, but rather a result of fluoroquinolone binding.[49] The proposed cooperativity is also questionable as Critchlow and Maxwell[48] found saturable binding at 2 quinolones per DNA binding site as opposed to 4 by Shen, while several groups have not observed cooperativity.[45, 46, 53] The NMR and MD results presented here indicate that the function of Mg(II) is to increase the affinity for groove binding, particularly minor groove binding, by electrostatic interaction with the phosphate backbone (**Papers II and III**).

On a molecular level it is seen that magnesium binds to the keto-carboxylate moiety of the quinolone skeleton, as expected from previous NMR and x-ray structures.[123] Surprisingly, Mg(II)-binding induces selective line broadening of the quinolone H2 and H5 signals in the NMR spectra. Mg(II)-binding to the phosphate groups of DNA and RNA is well known and the binding is a key factor in many enzyme mechanisms. Line broadening has, as far as we know, not been reported for these interactions. This is not strange as magnesium is

diamagnetic and not expected to induce line broadening for ^{1}H resonances. However, the natural abundance of the quadrupolar ^{25}Mg isotope (spin 5/2) is ~ 10%, and at stoichiometric ratio this could lead to quadrupolar relaxation of adjacent protons. Both the Mg(II)-binding to the nucleic acid phosphates and the Mg(II)-chelation of the keto-carboxyl moiety of quinolones, entail a 5-bond scalar coupling ($^{5}J_{Mg-H}$). Nevertheless, in the case of nucleic acids the scalar coupling is mediated through saturated bonds, while for quinolones, it is mediated through a conjugated, aromatic system. We suggest that the line broadening effect of magnesium(II) is due to the quadrupolar ^{25}Mg isotope. The unique chemical environment of the binding site in quinolones could be the reason why Mg(II)-induced line broadening is observed for quinolones, but not for other common Mg(II) interactions. None of the NMR studies on metal-fluoroquinolone complexes have reported values for line widths, but selective line broadening is observed for ciprofloxacin, levofloxacin and ofloxacin in our studies.

Binding preference, ss- or ds-DNA: Different preferences for ss- and ds-DNA have been reported without any apparent experimental differences to explain them. However, reports favouring binding to ss-DNA[43, 46, 50, 52, 61, 63] have typically lower fluoroquinolone concentrations than those needed for NMR experiments. The binding preference seems also to be sensitive to the ionic strength of the solution and the presence of divalent metal ions. Fluorescence experiments[52, 62, 124] indicated no preference for ss- or ds-DNA at intermediate to high salt concentration (> ~5 mM), while at low concentration (1.8 mM) or in the absence of NaCl, a ~4-5 fold preference for ss-DNA was observed. Surface plasmon resonance (SPR) measurements on DNA attached to sensor chips showed sequence-dependent binding to ss-DNA.[50] While the affinity for the single-stranded hexamer d(TGGCCT) was higher than for the corresponding double-stranded hairpins, the affinity for d(TAACCT) was lower than for it's corresponding double-stranded hairpin. In the same report, addition of Mg(II) ions increased the affinity for both the ss-DNA and the ds-DNA hairpins. Apparently, binding preference is dependent of several factors and particularly studies without Mg(II) give very limited information about the fluoroquinolone binding mechanisms. We found that at the present conditions, levo does not interact with ss-DNA in the presence or absence of Mg(II). The drug:Mg(II) ratio was similar to that of the SPR measurements and possibly the discrepancy arises from the different techniques used.

The NOE cross-peaks observed for cipro - ds-DNA and levo – ds-DNA binding are irrefutable evidence for significant interaction with ds-DNA. It is also seen that the presence of Mg(II) significantly enhances the binding affinity and that minimal distortion of the ds-DNA is required for the binding of quinolones. Our results are therefore contradictory to the Shen and Maxwell models that require an unwinding or distortion of the DNA in the vicinity of the DNA Gyrase cleavage site. Both models are based on results in the absence of Mg(II), again indicative of the important role of this metal ion. Interestingly, the only NMR study of quinolone binding to DNA in the presence of Mg(II)[58] showed binding preference to linear DNA over supercoiled plasmid DNA, in agreement with our results. The cellular fluoroquinolone:Mg(II) ratio is in the range 1:10 to 1:20, similar to the values used in the NMR experiments. This makes it plausible that the interactions observed in the NMR are relevant for the interactions taking place in the cell.

Our results did not show any clear sequence-dependent interaction with ds-DNA. In two other reports, Vilfan et al.[62] found preferential binding to poly[d(A-T)]•poly[d(A-T)] over poly[d(G-C)]•poly[d(G-C)], but the opposite was found in the study by Bailly et al.[61] It is difficult to make a direct comparison between the interaction of quinolones with polynucleotides and with the oligomers studied here.

Binding mode: groove, surface and/or intercalation: The NMR data shows that fluoroquinolone binds in the major and minor groove, to the terminal residues and by intercalation between GpG steps. Minor groove interaction is favoured at the terminal ends, consisting of 5´-CCTC, 5´-TATG and 5´-GATC for the duplexes investigated. Also the NMR study by Sandström et al.[64] strongly indicated minor groove binding, but major groove binding and intercalation could not be excluded. Molecular modelling and docking show optimal van der Waals complementarity of cipro and levo in the minor groove, similar to the model for norfloxacin binding to DNA.[51] Thus, the conformational fit in the minor groove seems to be a common feature for all fluoroquinolones. The possibility of surface binding cannot be ruled out, as a simple electrostatic interaction of Mg(II) with the DNA phosphate groups and random orientation of the fluoroquinolone molecule would be difficult to detect by NMR. The presence of multiple binding modes is in agreement with CD spectra of levo interaction with poly[d(G-C)·d(G-C)],[63] which showed a transition to multiple-site binding at a levo:base ratio of 1:5 similar to the ratio needed for intercalation in our studies. Also Son et al.[53] reported increased orientability at higher drug:DNA

concentrations in support of the presence of multiple binding modes. The use of a one-site binding model for the analysis of fluorescence and CD/LD data[52, 54, 61, 62] could be part of the reason why conflicting reports for the binding mode are given. Unfortunately, the NMR data cannot explain the mutually excluding binding preference reported from fluorescence (groove binding, not intercalation) and CD/LD (intercalation, not groove binding).

Our data suggests that while groove binding is the predominant interaction mode at low levo:DNA ratios, intercalation is an important binding mode at higher ratios. The relatively low intracellular drug concentration, ~0.1 mM,[56] suggests that high drug:DNA ratios are not readily achieved in the cell. However, localised quinolone-induced rearrangement on the enzyme DNA Gyrase can give rise to favourable interactions sites altering the binding affinity. The possibility of high drug:DNA ratio interaction, and thereby intercalation, should therefore not be disregarded. It is difficult to rationalise the minor groove binding of fluoroquinolones. The labile binding and intermediate affinity constant of fluoroquinolone to DNA suggest that the key to the bactericidal effect must lie within the interaction of the quinolone-Mg(II)-DNA complex with the DNA Gyrase enzyme.

3.2 Cisplatin Adducts on a GGG Sequence Within a DNA Double-stranded Decamer Studied by NMR Spectroscopy and Molecular Dynamics Simulations (paper IV)

In this paper the structural effects of adjacent guanine bases to the G*pG*-cisplatin adduct are investigated.

The structural perturbation caused by binding of platinum antitumor drugs to DNA has been shown to be specifically recognized by a number of cellular proteins, including HMGB proteins having function in chromatine organization or as transcription factors, repair proteins, or the TATA box binding protein.[96] It is believed that (some of) these recognition proteins mediate the cellular response which finally induces cell death by apoptosis or necrosis.[79] Relatively subtle changes in the adduct structure can affect the recognition and the biological effects in a major way.

A number of structural studies on cisplatin (*cis*-$[PtCl_2(NH_3)_2]$) adducts with duplex DNA have been reported,[97-99, 101, 103, 104, 125-128] all with the context -pyG*G*X- (py = pyrimidine and X = T, C, or A). The bases flanking a G*G* cross-link have been shown to have little effect on the major parameters defining the structural perturbation, the kink and unwinding angles,[129] except when the diamine has bulky substituents.[130] We decided to investigate the influence of having a guanine on the 3´ side of the G*G* cross-link to see if this was in accord with the observations for pyG*G* adducts.

The non-palindromic duplex $[d(G_1C_2C_3G_4G_5G_6T_7C_8G_9C_{10})\cdot d(G_{11}C_{12}G_{13}A_{14}C_{15}C_{16}C_{17}G_{18}G_{19}C_{20})]$ (GGG), was platinated using ^{15}N-labeled *cis*-$[PtCl_2(NH_3)_2]$. The sequence was chosen because it is almost identical to the duplex $[d(G_1C_2C_3G^*_4G^*_5A_6T_7C_8G_9C_{10})\cdot d(G_{11}C_{12}G_{13}A_{14}T_{15}C_{16}C_{17}G_{18}G_{19}C_{20})]$ (G*G*A) (GC pair exchanged by an AT pair) studied previously.[98, 118] Applying recently improved HPLC protocols for the separation of platinated oligonucleotides,[131] the two adducts, 1,2 and 2,3 cisplatin-GGG, were separated (see Figure 3.2.1) and the purified 1,2 adduct was annealed with its complementary strand yielding a B-DNA-like duplex (G*G*G). The structure was then investigated by 1D and 2D NMR (NOESY, DQF-COSY, TOCSY, ^{15}N-^{1}H HSQC and ^{31}P-^{1}H HETCOR) and molecular modelling (MD).

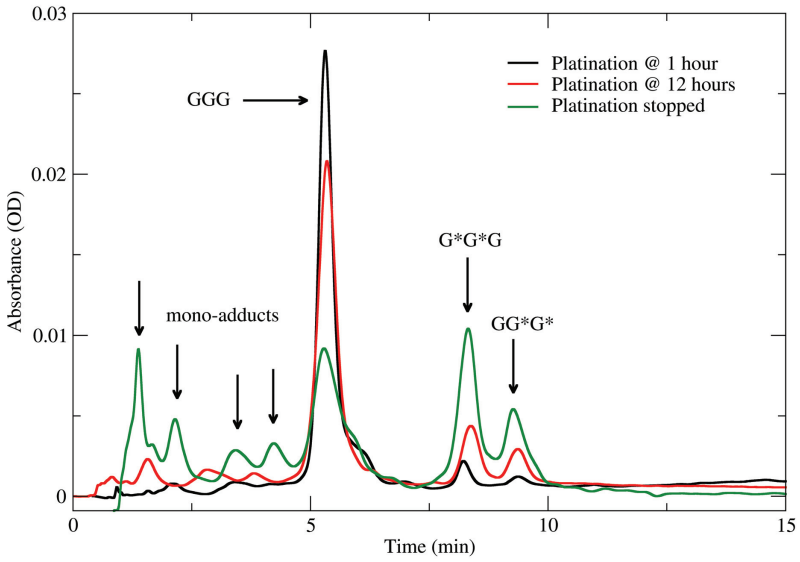

Figure 3.2.1. HPLC chromatogram showing the changes in peak intensities as a function of time. Samples were taken from the reaction mixture of single-stranded 5´-d(GCCGGGTCCGC) –3´ and ^{15}N-labelled cisplatin.

*The influence of a G on the 3´-side of the G*G* cross-link*

The NMR results indicate that the chemical shifts of G*G*G show all the typical features of platinated pyG*G* duplexes.[105] In particular, the two downfield-shifted H8 resonances of G*4 and G*5 confirm that these bases are platinated and their chemical shifts are characteristic of all pyG*G* adducts characterized so far (i.e., ~8.7 ppm for the 5´ G* and 8.0-8.4 ppm for the 3´ G*, see also discussion in chapter 1.3.3 and Table 3.2.1). The ^{31}P spectrum shows that the phosphate group between the two platinated G*´s is shifted substantially downfield (-3.12 ppm). The ^{1}H resonance of the C-H2´ on the 5´-side of G*G* is strongly upfield shifted (1.52 ppm) and is reasonably well correlated with the H2´ of the cytidine complementary to 5´ G*.[118] The 2D NOESY spectra show a strong G*4-(H8-H3´) cross-peak, indicative of an N sugar for the 5´ G*. A complete sequential walk could be performed for both strands with the exception of the C3-G*4 and G*4-G*5 steps. However, these steps could be easily followed in the H2´/2´´-H68 region, thus confirming that there was no break in the sequence. All these spectral features suggest that the G*G*G adduct is similar to that of pyG*G*X (X = A, C, T) reported.[97-99, 101, 102, 104] The G*G*G shifts were shown to be virtually superimposable to the shifts observed for G*G*A, indicating that the change of a purine for another purine has no large effects on the structure of the adduct.

Table 3.2.1. Chemical shifts of platinated duplexes and their relative shifts compared to their unplatinated duplexes.

	CG*G*T	Δδ	TG*G*T	Δδ	CG*G*A	Δδ	CG*G*G	Δδ	GG*G*T	Δδ
X-H2´	1.46	-0.54	1.37	-0.55	1.58	-0.47	1.52	-0.47	2.56	-0.10
5´ G*-H8	8.73	1.13	8.64	0.89	8.70	0.73	8.71	0.88	8.29	0.62
3´ G*-H8	8.02	0.41	8.08	0.52	8.36	0.39	8.37	0.70	7.95	0.42

Only three cisplatin adducts to dsDNA have reported shifts for the unplatinated sequence and are included in the table. These are: CG*G*T (den Hartog et al.[97]); TG*G*T (Parkinson et al.[103]); CG*G*A (Herman et al.[98]; CG*G*G and GG*G*T (this study, paper IV). Δδ = Shift difference of platinated to unplatinated duplex. X-H2´ is for the nucleotide 5´ to the 5´ G*.

These observations raise some interesting questions regarded the influence of flanking bases on G*G* adducts. The available NMR spectra[97-99, 101, 103, 104] show that the 5´ G*-H8 signal has an absolute shift in the range 8.66 - 8.76 ppm, while the 3´ G*-H8 signal is in the range 8.02 - 8.39 ppm. Table 3.2.1 summarizes the relative shifts for three platinated duplexes where data for the unplatinated strand was available, in addition to shifts reported in this thesis. It is seen that the variation in the magnitude of the relative downfield shift for 5´ G*-H8 (~0.4 ppm), in pyG*G*X adducts, is much larger than the variation in the absolute shift (~0.1 ppm). It is plausible to assume that the G*-Pt-G* adduct is rigid and that the variations in G* shifts are determined by the variations in the influence of the flanking bases. This is supported by the molecular modelling, which shows that the 5´ G*-H8 is outside the shielding cone of the 5´-flanking cytosine base for the complete duration of the simulation.[118] This suggests that the conformation of the pyG*G* context is similar for all the adducts investigated and that the GG*G* context is essentially different.

However, the variations in the absolute and the relative shifts of the 3´ G*-H8 both relatively large (~0.4 and ~0.3 ppm, respectively), which suggests that the 3´-flanking base to the G*G* cross-link has a larger influence on the chemical shift than the 5´-flanking base. The absolute shifts for the 3´ G*-H8 are similar for NG*G*T (N=any nucleotide), 8.02 - 8.19 ppm, and for NG*G*X (X=C,A,G), 8.36 – 8.39 ppm. This difference does not necessarily originate from a different conformation of the G*G*N context, but could be a consequence of the lesser ring current effect of thymine compared to C, A or G.[132]

NOESY data in combination with J-coupling data from DQF-COSY spectra show that the 5´ G* has an N sugar and the 5´-CG* predominantly N sugar. The three cytosines

complementary to the 5´ G*G*G-3´ sequence show N↔E↔S, N↔S and S for 5´-**C_{15}**$C_{16}C_{17}$-3´, 5´-C_{15}**C_{16}**C_{17}-3´, 5´-$C_{15}C_{16}$**C_{17}**-3´, respectively. The indication of E sugar for C15 is particularly interesting as E sugars are normally not considered for sugar pucker characterisation. The inclusion of E sugar pucker in the model was spawned by the observation of ~2 ns recurring E sugar transitions in the MD simulation (*vide infra*). Djuranovic and Hartmann[107] investigated a large number of x-ray structures and found that E sugars are quite frequent in B-DNA, 7 - 30 % depending on nucleotide, and that the E sugars repucker upon protein binding. This suggests that E sugars transitions could also be important in characterising structural perturbations following drug-DNA interactions.

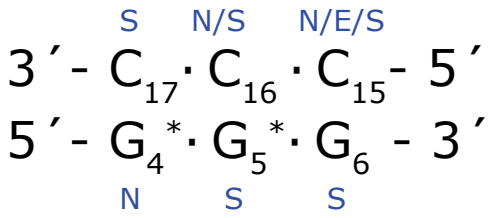

Figure 3.2.2 Sugar pucker conformations for the central trinucleotide of the G*G*G duplex adduct.

Molecular Dynamics simulations

Extensive unrestrained molecular dynamics (MD) simulations of G*G*G were performed using Amber6 and the parm98 force field extended by parameters describing the platinum coordination (as described by Elizondo-Riojas & Kozelka[118]). The first 10 ns of the 20 ns production period were discarded due to the observation of reversible G*4 sugar pucker transitions to S. These transitions were an obvious artefact since the NMR data showed virtually 100% N pucker, in accordance with all the available data on G*pG*-platinated DNA duplexes. This observation shows that the S-shifted N↔S equilibrium in parm98 overrides the N-shifted equilibrium specific to the 5´ G* introduced in the extended Pt parameters by Elizondo-Riojas and Kozelka. This should be accounted for in new versions of the cisplatin-G*G* adduct parameters.

Average distances from the MD were compared with the average distances derived from the NOESY data. The distances were found to be in good agreement, the average difference was 0.44 (±0.35) Å. More importantly, the average difference for the interaction site, defined as the context 5´-CG*G*GT-3´ and the complementary 5´-ACCCG-3´, was

0.41 (±0.29) Å, i.e. within the boundaries for experimentally derived NMR distances (±0.60 Å).

The G*G*G duplex has a B-DNA-like conformation, the helix kinked 67±9° towards the major groove, localized at the platination site. The roll between G*4 and G*5 is 74±3°. Sugar puckers are all 96-100 % S, except C3 and G*4 having 22 and 21 % S, respectively, and C15 and C16 having 66 and 5 % S, respectively. The NMR data indicated ~40 % S for C3 and an N↔S equilibrium shifted towards S for C16. One reason for this discrepancy with the MD is that both C16 and C3 suffer from cross-peak overlap in the NOESY spectra, resulting in larger uncertainties for these sugar puckers.

MD simulations for G*G*A[118] indicated that the A6pT7 step adopts partly a BII conformation stabilized by a hydrogen bond between an NH_3 ligand of platinum and the A6-N7 atom. The substitution of 3´ G by 3´-A was expected to strengthen this bond due to the higher basicity of the G6-N7. However, the MD simulations for G*G*G show a BI conformation for the G6pT7 step and the ^{31}P NMR spectrum indicates the same. These observations therefore do not support the hypothesis of a Pt-NH_3↔pu-N7 hydrogen bond stabilization of the G*G*-cisplatin adduct.

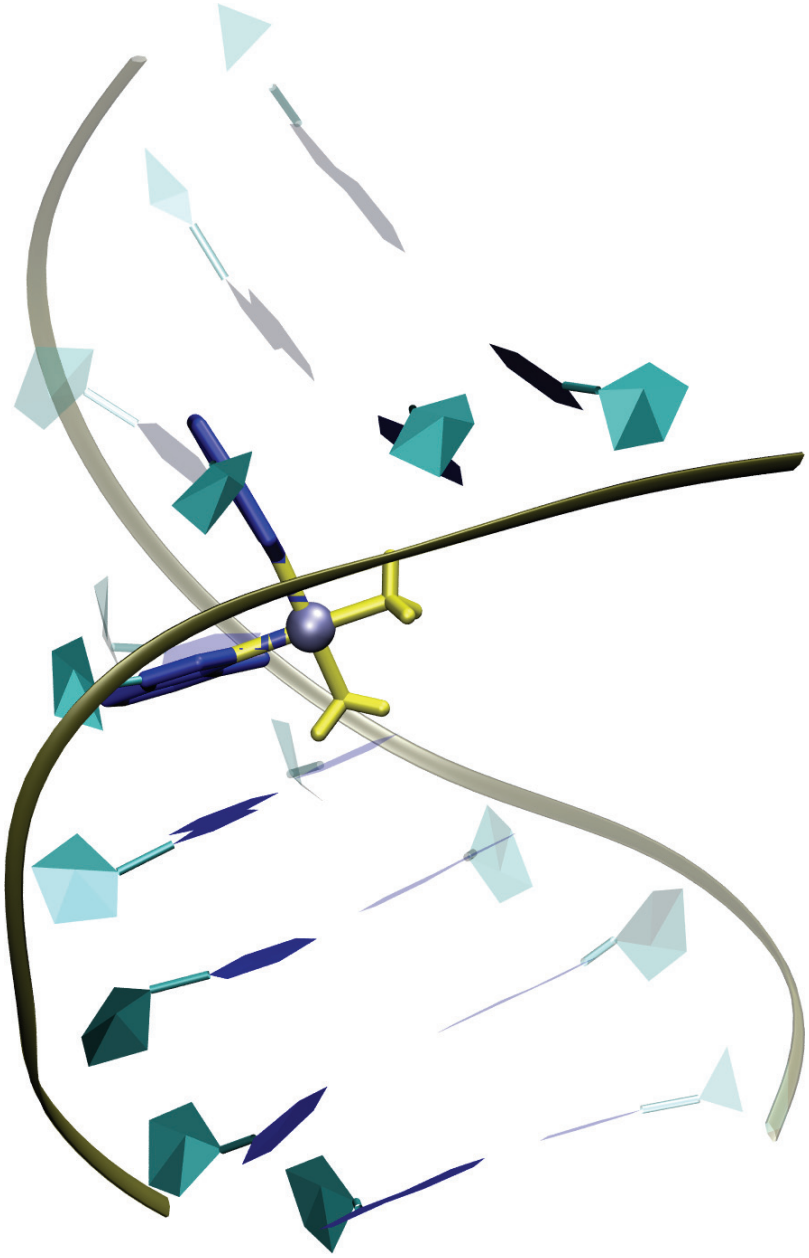

Figure 3.2.3. Structure of the G*G*G oligomer averaged over 10 ns and subsequently energy minimised. Guanine bases are represented in blue, platinum in grey and the amines in yellow.

*Isomerization reaction from G*G*G to GG*G**

While the NMR analysis was in progress for the duplex, it became evident that the sample contained not one but two platinated DNA duplex species. Nine days after annealing the platinated strand, one major (~70 %) and one minor (~30 %) species were observed. The NMR data showed (*vide supra*) that an unprecedented isomerization reaction had occurred, from G*4G*5 (major) to G*5G*6 (minor), reaching a final equilibrium of approximately 40:60 (G*4G*5:G*5G*6) after 200-300 days.

The observed isomerization on the duplex adduct indicates that the previous dogma of non-labile cisplatin binding to guanine N7 should be reconsidered. The fact that only 5´-pyGGX-3´ sequences (py = pyrimidine and X = C, T or A) have been studied so far, explains why this has not been observed previously. The isomerization reaction would most likely involve a G-N7-cisplatin monoadduct as the transition state. Ring closure for such monoadducts was found to be faster towards the 5´ side than the 3´ side,[133] which would result in predominantly 5´-G*G*G-3´ adducts. The present results therefore suggest that although the 5´-G*G*G-3´ adduct is the kinetically favoured adduct, the 5´-GG*G*-3´ adduct is the more thermodynamically stable.

*Influence of a G on the 5´side of the G*G* cross-link*

The chemical shifts for GG*G* shows some important differences to all the pyG*G* containing duplexes analysed by Marzilli et al.[134] as well as by Elizondo-Riojas and Kozelka[118] and found to be mutually similar. The 5´ G*H8 resonance in GG*G* experience a significantly lower downfield shift than what is common for platinated duplexes,[97, 98, 103] possibly due to shielding by the ring current of the guanine G4. The nucleotide 5´ to the cross-link (i.e. G4) lacks the strongly upfield-shifted H2´ signal of pyG*G* adducts (~ -0.50 ppm). This particular shift has been shown to originate from the ring current of the 5´ G* into whose shielding cone the H2´ proton penetrates.[118] A strong H2´-H8 and a moderate H3´-H8 cross-peak for G4 suggests an S conformation for the sugar, whereas in the pyG*G* adducts, this nucleotide has partly or entirely N pucker. The sum of the NMR data indicate that the XpG* step is significantly different in GG*G*, which also implies that the dynamics of the corresponding XY base pair in 5´-**X**G*-3´/5´-C**Y**-3´ is different. The ^{31}P spectrum shows that only the shift of G5*pG6* deviates from the normal observed range (~ - 4.0 to - 4.2 ppm). This signal is downfield shifted 0.8 ppm, similar to that of all G*pG* adducts studied so far.

.

$$\begin{array}{l} \overset{\text{S}\quad\ \text{S}\quad\ \text{N}\quad\ \text{N/S}}{3'-C_{17}\cdot C_{16}\cdot C_{15}\cdot A_{14}-5'} \\ 5'-G_{4}\cdot G_{5}^{*}\cdot G_{6}^{*}\cdot T_{7}-3' \\ \underset{\text{S}\quad\ \text{N}\quad\ \text{S}\quad\ \text{S}}{} \end{array}$$

Figure 3.2.4. Sugar pucker conformations for the central of the GG*G* duplex adduct

Interestingly, the same deviations from the general spectral features of pyG*G* duplex adducts were recently reported for the duplex [d(CCTCAG*G*CCTCC)·

d(GGAGGCCTGAGG)] cross-linked at G*pG* by $Pt(DACH)^{2+}$ (DACH = trans-1,2-diaminocyclohexane).[135] The differences were ascribed to the presence of the DACH ligand, which is sterically more demanding than the two NH_3 groups of cisplatin. Molecular models of the AG*G*-Pt(DACH) adduct showed a significantly smaller kink angle than the models proposed previously. However, comparing the NMR features of AG*G*-Pt(DACH) with those of GG*G*, we propose that the factor responsible for the unusual spectral features is the purine 5´ to the G*pG* cross-link, rather than the diamine ligand.

Conclusions

The isomerization reaction enabled us to compare the effects of guanine flanking bases on both the 3´ and the 5´ side of the G*G* cross-link, as compared to pyrimidine flanking bases. It has been shown that a 3´ flanking guanine has little influence on the G*G* cross-link, while having a flanking guanine on the 5´ side induces significant structural perturbations. The context -GG*G*T- is basically similar in structure to the general -pyG*Gpy- context, but the 5´ XpG* step is different in both structure and dynamics. The fact that the isomerization reaction took place suggests that the cisPt - GN7 bond is labile. This would implicate that models used to describe protein interaction with cisplatin-DNA cross-links should be re-evaluated.

4 Conclusions

The conclusions of this work are divided into two categories according to the drug investigated.

Fluoroquinolones:

- The orientation of the oxazine methyl group of ofloxacin alters the solid and solution state properties for this fluoroquinolone.
- Levofloxacin did not show significant interaction with single-stranded DNA in the presence or absence of Mg(II).
- In the presence of Mg(II), ciprofloxacin and levofloxacin bind to the major and minor groove of double-stranded DNA. In the absence of Mg(II) the binding is less specific or is not observed, for ciprofloxacin and levofloxacin, respectively.
- Molecular modelling showed that minor groove binding was favourable due to the remarkable complementarity of fluoroquinolone and DNA van der Waals surfaces.
- Ciprofloxacin and levofloxacin show a high degree of interaction with the terminal base pairs.
- At higher ratios of levofloxacin:ds-DNA (> 5:1), levofloxacin can intercalate between central GpG base steps.

Cisplatin:

- The NMR features of G*G*G were found to be similar to those of DNA duplexes cross-linked by cisplatin at a pyG*G*X site (X = C, T, A), indicating that a guanine 3´ to the G*G*-Pt cross-link does not particularly affect the structure.
- An unprecedented isomerization reaction on intact duplex state between 1,2 and 2,3 platination lead to a 40:60 equilibrium between G*G*G and GG*G* species.
- The presence of a guanine 5´ to the G*G* cross-link induces structural perturbations significantly different from pyG*G* sequences.

5 Suggestions for further work

Suggestions for further work are divided into two categories according to the drug investigated.

Fluoroquinolones:

- A systematic investigation of the self-association properties would give answers to the probability of cooperativity in the interaction of fluoroquinolones with DNA and the DNA – DNA Gyrase complex.
- A systematic investigation of the influence of ionic strength, type of salt and pH on the binding affinity of fluoroquinolones to DNA and the DNA – DNA Gyrase complex could give more information on the protonation state(s) for the active fluoroquinolone species.
- Investigate the role of cooperativity by studying the binding affinity of mixtures of fluoroquinolones, e.g. ratios of ciprofloxacin:levofloxacin, for DNA and DNA Gyrase. Possible changes in MIC due to the mixtures should be checked.
- A high-field NMR and a high-resolution x-ray structure of the DNA Gyrase - DNA complex are necessities for a real advance in the elucidation of the molecular mechanisms for this fascinating enzyme. The NMR structure could be achieved by high-concentration, selectively radiolabeled samples on high-field 800 or 900 MHz instruments using multinuclear (^{1}H, ^{13}C, ^{15}N, ^{19}F, ^{31}P), multidimensional experiments.
- An ^{15}N-labelled fluoroquinolone sample would allow the kinetics of fluoroquinolone binding to the DNA – DNA Gyrase complex to be determined. Selective labelling of DNA and DNA Gyrase could also give information about the interaction site through dipole-dipole couplings.
- The use of EPR with Mg(II) substituted with Mn(II) could give information on the role of Mg(II) in the blocking mechanism of fluoroquinolones in the ternary DNA – fluoroquinolone – DNA Gyrase complex.

Cisplatin:

- A high-resolution NMR study of HPLC-separated G*G*G and GG*G* adducts should be performed with ^{15}N and ^{13}C labelled samples for improved structural

characterization. This could give answers to the structural differences between the two types of adducts.

- A high-resolution x-ray structure would be complementary to the NMR structure.
- Combined use of gel electrophoresis and ^{15}N-NMR could give better values for the migration kinetics.
- The repair enzyme efficiency for G*G*G and GG*G* adducts should be measured. This could tell whether the different structure influences the anticancer activity.
- Improved force field parameters describing the G*G* adduct would allow better MD. High-resolution structures from NMR and/or x-ray could form the basis for optimalised parameters for the different structures.

References

[1] O. T. Avery, C. Macleod and M. McCarthy, *J. Exp. Med.* **1944**, *79*, 137-157.
[2] E. Chargaff, *Experientia* **1950**, *6*, 201-209.
[3] J. D. Watson and F. H. C. Crick, *Nature* **1953**, *171*, 737-738.
[4] A. H. J. Wang, G. J. Quigley, F. J. Kolpak, J. L. Crawford, J. H. Van Boom, G. Van der Marel and A. Rich, *Nature* **1979**, *282*, 680-686.
[5] R. Wing, H. Drew, T. Takano, C. Broka, S. Tanaka, K. Itakura and R. E. Dickerson, *Nature* **1980**, *287*, 755-758.
[6] P. M. Takahara, A. C. Rosenzweig, C. A. Frederick and S. J. Lippard, *Nature* **1995**, *377*, 649-652.
[7] H. Sugiyama and I. Saito, *J. Am. Chem. Soc.* **1996**, *118*, 7063-7068.
[8] A. Rich, A. Nordheim and A. H. J. Wang, *Annu. Rev. Biochem.* **1984**, *53*, 791-846.
[9] M. S. Searle, *Prog. Nucl. Magn. Reson. Spectrosc.* **1993**, *25*, 403-480.
[10] M. S. Searle, J. G. Hall, W. A. Denny and L. P. G. Wakelin, *Biochemistry* **1988**, *27*, 4340-4349.
[11] M. S. Searle, W. Bicknell, L. P. G. Wakelin and W. A. Denny, *Nucleic Acids Res.* **1991**, *19*, 2897-2906.
[12] D. Y. Sun, M. Hansen, J. J. Clement and L. H. Hurley, *Biochemistry* **1993**, *32*, 8068-8074.
[13] T. K. Chiu and R. E. Dickerson, *J. Mol. Biol.* **2000**, *301*, 915-945.
[14] A. Maxwell, *Trends Microbiol.* **1997**, *5*, 102-109.
[15] V. T. Andriole in *The Quinolones* (Ed. V. T. Andriole), Academic Press, San Diego, California, **2000**.
[16] D. C. Hooper, *Quinolone antimicrobial agents* (Eds. D. C. Hooper and E. Rubinstein), ASM Press, Washington D.C., **2003**.
[17] L. A. Mitscher, *Chem. Rev.* **2005**, *105*, 559-592.
[18] G. Y. Lesher, M. D. Gruett, E. J. Froelich, R. P. Brundage and J. H. Bailey, *Journal of Medicinal & Pharmaceutical Chemistry* **1962**, *5*, 1063-&.
[19] T. D. Gootz and K. E. Brighty in *The Quinolonones*, (Ed. V. T. Andriole), Academic Press, San Diego, **1998**, pp. 29-80.
[20] K. N. Kreuzer and N. R. Cozzarelli, *J. Bacteriol.* **1979**, *140*, 424-435.
[21] S. J. Froelich-Ammon and N. Osheroff, *J. Biol. Chem.* **1995**, *270*, 21429-21432.
[22] J. H. M. Cabral, A. P. Jackson, C. V. Smith, N. Shikotra, A. Maxwell and R. C. Liddington, *Nature* **1997**, *388*, 903-906.
[23] L. Klevan and J. C. Wang, *Biochemistry* **1980**, *19*, 5229-5234.
[24] S. Krueger, G. Zaccai, A. Wlodawer, J. Langowski, M. Odea, A. Maxwell and M. Gellert, *J. Mol. Biol.* **1990**, *211*, 211-220.
[25] P. Hallett and A. Maxwell, *Antimicrob. Agents Chemother.* **1991**, *35*, 335-340.
[26] H. Gmunder, K. Kuratli and W. Keck, *Antimicrob. Agents Chemother.* **1995**, *39*, 163-169.
[27] M. Couturier, E. Bahassi and L. Van Melderen, *Trends Microbiol.* **1998**, *6*, 269-275.

[28] J. Gore, Z. Bryant, M. D. Stone, M. N. Nollmann, N. R. Cozzarelli and C. Bustamante, *Nature* **2006**, *439*, 100-104.
[29] A. Morrison and N. R. Cozzarelli, *Cell* **1979**, *17*, 175-184.
[30] M. Q. Zhang and A. Haemers, *Pharmazie* **1991**, *46*, 687-700.
[31] T. D. Gootz and K. E. Brighty, *Med. Res. Rev.* **1996**, *16*, 433-486.
[32] B. Llorente, F. Leclerc and R. Cedergren, *Bioorg. Med. Chem.* **1996**, *4*, 61-71.
[33] F. Van Bambeke, J. M. Michot, J. Van Eldere and P. M. Tulkens, *Clinical Microbiology and Infection* **2005**, *11*, 256-280.
[34] D. L. Ross and C. M. Riley, *J. Pharm. Biomed. Anal.* **1994**, *12*, 1325-1331.
[35] A. Sugino, C. L. Peebles, K. N. Kreuzer and N. R. Cozzarelli, *Proc. Natl. Acad. Sci. U. S. A.* **1977**, *74*, 4767-4771.
[36] Y. H. Hsiang, M. G. Lihou and L. F. Liu, *Cancer Res.* **1989**, *49*, 5077-5082.
[37] Y. Pommier, F. Leteurtre, M. R. Fesen, A. Fujimori, R. Bertrand, E. Solary, G. Kohlhagen and K. W. Kohn, *Cancer Invest.* **1994**, *12*, 530-542.
[38] L. L. Shen and A. G. Pernet, *Proc. Natl. Acad. Sci. U. S. A.* **1985**, *82*, 307-311.
[39] L. L. Shen and D. T. W. Chu, *Curr. Pharm. Des.* **1996**, *2*, 195-208.
[40] I. Morrissey, K. Hoshino, K. Sato, A. Yoshida, I. Hayakawa, M. G. Bures and L. L. Shen, *Antimicrob. Agents Chemother.* **1996**, *40*, 1775-1784.
[41] L. L. Shen, L. A. Mitscher, P. N. Sharma, T. J. Odonnell, D. W. T. Chu, C. S. Cooper, T. Rosen and A. G. Pernet, *Biochemistry* **1989**, *28*, 3886-3894.
[42] L. L. Shen, W. E. Kohlbrenner, D. Weigl and J. Baranowski, *J. Biol. Chem.* **1989**, *264*, 2973-2978.
[43] L. L. Shen, J. Baranowski and A. G. Pernet, *Biochemistry* **1989**, *28*, 3879-3885.
[44] L. L. Shen, J. Baranowski and T. Wai, *J. Cell. Biochem.* **1986**, 203-203.
[45] G. Palu, S. Valisena, G. Ciarrocchi, B. Gatto and M. Palumbo, *Proc. Natl. Acad. Sci. U. S. A.* **1992**, *89*, 9671-9675.
[46] C. Sissi, M. Andreolli, V. Cecchetti, A. Fravolini, B. Gatto and M. Palumbo, *Bioorg. Med. Chem.* **1998**, *6*, 1555-1561.
[47] C. J. R. Willmott and A. Maxwell, *Antimicrob. Agents Chemother.* **1993**, *37*, 126-127.
[48] S. E. Critchlow and A. Maxwell, *Biochemistry* **1996**, *35*, 7387-7393.
[49] S. C. Kampranis and A. Maxwell, *J. Biol. Chem.* **1998**, *273*, 22615-22626.
[50] C. G. Noble, F. M. Barnard and A. Maxwell, *Antimicrob. Agents Chemother.* **2003**, *47*, 854-862.
[51] H. M. Lee, J. K. Kim and S. K. Kim, *J. Biomol. Struct. Dyn.* **2002**, *19*, 1083-1091.
[52] G. S. Son, J. A. Yeo, J. M. Kim, S. K. Kim, H. R. Moon and W. Nam, *Biophys. Chem.* **1998**, *74*, 225-236.
[53] G. S. Son, J. A. Yeo, M. S. Kim, S. K. Kim, A. Holmen, B. Akerman and B. Norden, *J. Am. Chem. Soc.* **1998**, *120*, 6451-6457.
[54] E. J. Lee, J. A. Yeo, C. B. Cho, G. J. Lee, S. W. Han and S. K. Kim, *Eur. J. Biochem.* **2000**, *267*, 6018-6024.
[55] E. J. Lee, J. A. Yeo, K. Jung, H. J. Hwangbo, G. J. Lee and S. K. Kim, *Arch. Biochem. Biophys.* **2001**, *395*, 21-24.

[56] S. Lecomte, M. H. Baron, M. T. Chenon, C. Coupry and N. J. Moreau, *Antimicrob. Agents Chemother.* **1994**, *38*, 2810-2816.
[57] S. Lecomte, X. Tabary, N. J. Moreau and M. T. Chenon, *Magn. Reson. Chem.* **1996**, *34*, 458-466.
[58] S. Lecomte, N. J. Moreau and M. T. Chenon, *Int. J. Pharm.* **1998**, *164*, 57-65.
[59] S. Tornaletti and A. M. Pedrini, *Biochim. Biophys. Acta* **1988**, *949*, 279-287.
[60] L. L. Shen, J. Baranowski, T. Wai, D. T. W. Chu and A. G. Pernet in *International Telesymposium on Quinolones*, (Ed. P. B. Fernandes), J.R. Prous Science Publishers, Barcelona, **1989**, pp. 159-170.
[61] C. Bailly, P. Colson and C. Houssier, *Biochem. Biophys. Res. Commun.* **1998**, *243*, 844-848.
[62] I. D. Vilfan, P. Drevensek, I. Turel and N. P. Ulrih, *Biochim. Biophys. Acta - Gene Struct. Expr.* **2003**, *1628*, 111-122.
[63] H. J. Hwangbo, B. H. Yun, J. S. Cha, D. Y. Kwon and S. K. Kim, *Eur. J. Pharm. Sci.* **2003**, *18*, 197-203.
[64] K. Sandstrom, S. Warmlander, M. Leijon and A. Graslund, *Biochem. Biophys. Res. Commun.* **2003**, *304*, 55-59.
[65] N. X. Chin and H. C. Neu, *Antimicrob. Agents Chemother.* **1983**, *24*, 754-763.
[66] M. L. J. Moncany and E. Kellenberger, *Experientia* **1981**, *37*, 846-847.
[67] C. F. Chang, H. Shuman and A. P. Somlyo, *J. Bacteriol.* **1986**, *167*, 935-939.
[68] T. Alatossava, H. Jutte, A. Kuhn and E. Kellenberger, *J. Bacteriol.* **1985**, *162*, 413-419.
[69] M. D. Snavely, *Met. Ions Biol. Syst.* **1990**, *26*, 155-175.
[70] J. E. Lusk and E. P. Kennedy, *J. Biol. Chem.* **1969**, *244*, 1653.
[71] B. Rosenberg, L. Van Camp and T. Krigas, *Nature* **1965**, *205*, 698-699.
[72] B. Rosenberg, L. Van Camp, J. E. Trosko and V. H. Mansoui, *Nature* **1969**, *222*, 385-386.
[73] K. Siafaca in *Oncology Trends Product Markets – Part I, Future Oncology*, New Medicine Inc., Lake Forest, CA, **1999**, pp. 1045-1071.
[74] P. J. Loehrer and L. H. Einhorn, *Ann. Intern. Med.* **1984**, *100*, 704-713.
[75] H. M. Keys, B. N. Bundy, F. B. Stehman, L. I. Muderspach, W. E. Chafe, C. L. Suggs, J. L. Walker and D. Gersell, *N. Engl. J. Med.* **1999**, *340*, 1154-1161.
[76] M. Morris, P. J. Eifel, J. D. Lu, P. W. Grigsby, C. Levenback, R. E. Stevens, M. Rotman, D. M. Gershenson and D. G. Mutch, *N. Engl. J. Med.* **1999**, *340*, 1137-1143.
[77] P. G. Rose, B. N. Bundy, E. B. Watkins, J. T. Thigpen, G. Deppe, M. A. Maiman, D. L. Clarke-Pearson and S. Insalaco, *N. Engl. J. Med.* **1999**, *340*, 1144-1153.
[78] G. J. Bosl and R. J. Motzer, *N. Engl. J. Med.* **1997**, *337*, 242-253.
[79] J. R. Jamieson and S. J. Lippard, *Chem. Rev.* **1999**, *99*, 2467-2497.
[80] S. Mansy, B. Rosenberg and A. J. Thomson, *J. Am. Chem. Soc.* **1973**, *95*, 1633-1640.
[81] A. B. Robins, *Chem. Biol. Interact.* **1973**, *6*, 35-45.
[82] A. B. Robins, *Chem. Biol. Interact.* **1973**, *7*, 11-16.

[83] A. M. J. Fichtinger-Schepman, A. T. van Oosterom, P. H. M. Lohman and F. Berends, *Cancer Res.* **1987**, *47*, 3000-3004.
[84] A. M. J. Fichtinger-Schepman, J. L. van der Veer, J. H. J. Den Hartog, P. H. M. Lohman and J. Reedijk, *Biochemistry* **1985**, *24*, 707-713.
[85] V. Brabec in *DNA modifications by antitumor platinum and ruthenium compounds: Their recognition and repair*, *Vol. 71* **2002**, pp. 1-68.
[86] C. A. Lepre, K. G. Strothkamp and S. J. Lippard, *Biochemistry* **1987**, *26*, 5651-5657.
[87] A. Eastman, M. M. Jennerwein and D. L. Nagel, *Chem. Biol. Interact.* **1988**, *67*, 71-80.
[88] F. Reeder, J. Kozelka and J.-C. Chottard, *Inorg. Chem.* **1996**, *35*, 1413-1415.
[89] F. Reeder, F. Gonnet, J. Kozelka and J. C. Chottard, *Chem. Eur. J.* **1996**, *2*, 1068-1076.
[90] S. J. Berners-Price, K. J. Barnham, U. Frey and P. J. Sadler, *Chem. Eur. J.* **1996**, *2*, 1283-1291.
[91] S. K. C. Elmroth and S. J. Lippard, *Inorg. Chem.* **1995**, *34*, 5234-5243.
[92] F. Legendre, V. Bas, J. Kozelka and J.-C. Chottard, *Chem. Eur. J.* **2000**, *6*, 2002-2010.
[93] M. S. Davies, S. J. Berners-Price and T. W. Hambley, *Inorg. Chem.* **2000**, *39*, 5603-5613.
[94] F. Legendre, J. Kozelka and J.-C. Chottard, *Inorg. Chem.* **1998**, *37*, 3964-3967.
[95] M. S. Davies, S. J. Berners-Price and T. W. Hambley, *J. Am. Chem. Soc.* **1998**, *120*, 11380-11390.
[96] D. B. Zamble and S. J. Lippard in *The Response of Cellular Proteins to Cisplatin-Damaged DNA*, (Ed. B. Lippert), Verlag Helvetica Chimica Acta, Zürich, **1999**, pp. 73-110.
[97] J. H. J. den Hartog, C. Altona, J. H. van Boom, G. A. van der Marel, C. A. G. Haasnoot and J. Reedijk, *J. Biomol. Struct. Dyn.* **1985**, *2*, 1137-1155.
[98] F. Herman, J. Kozelka, V. Stoven, E. Guittet, J.-P. Girault, T. Huynh-Dinh, J. Igolen, J.-Y. Lallemand and J.-C. Chottard, *Eur. J. Biochem.* **1990**, *194*, 119-133.
[99] D. Yang, S. S. G. E. van Boom, J. Reedijk, J. H. van Boom and A. H.-J. Wang, *Biochemistry* **1995**, *34*, 12912-12920.
[100] M.-H. Fouchet, E. Guittet, J. A. H. Cognet, J. Kozelka, C. Gauthier, M. Le Bret, K. Zimmermann and J.-C. Chottard, *J. Biol. Inorg. Chem.* **1997**, *2*, 83-92.
[101] A. Gelasco and S. J. Lippard, *Biochemistry* **1998**, *37*, 9230-9239.
[102] S. U. Dunham, S. U. Dunham, C. J. Turner and S. J. Lippard, *J. Am. Chem. Soc.* **1998**, *120*, 5395-5406.
[103] J. A. Parkinson, Y. Chen, Z. Guo, S. J. Berners-Price, T. Brown and P. J. Sadler, *Chem. Eur. J.* **2000**, *6*, 3636-3644.
[104] L. G. Marzilli, J. S. Saad, Z. Kuklenyik, K. A. Keating and Y. Xu, *J. Am. Chem. Soc.* **2001**, *123*, 2764-2770.
[105] S. O. Ano, Z. Kuklenyik and L. G. Marzilli in *Structure and Dynamics of Pt Anticancer Drug Adducts from Nucleotides to Oligonucleotides as Revealed by NMR Methods*, (Ed. B. Lippert), Verlag Helvetica Chimica Acta, Zürich, **1999**, pp. 247-291.

[106] S. Arnott and D. W. L. Hukins, *Biochem. Biophys. Res. Comm.* **1972**, *47*, 1504-1509.
[107] D. Djuranovic and B. Hartmann, *J. Biomol. Struct. Dyn.* **2003**, *20*, 771-788.
[108] T. P. Kline, L. G. Marzilli, D. Live and G. Zon, *Biochem. Pharmacol.* **1990**, *40*, 97-113.
[109] P. G. Yohannes, G. Zon, P. W. Doetsch and L. G. Marzilli, *J. Am. Chem. Soc.* **1993**, *115*, 5105-5110.
[110] M. Iwamoto, S. Mukundan, Jr. and L. G. Marzilli, *J. Am. Chem. Soc.* **1994**, *116*, 6238-6244.
[111] J. M. Villanueva, X. Jia, P. G. Yohannes, P. W. Doetsch and L. G. Marzilli, *Inorg. Chem.* **1999**, *38*, 6069-6080.
[112] M.-A. Elizondo-Riojas, F. Gonnet, P. Augé-Barrere-Mazouat, F. Allain, J. Bergès, R. Attias, J.-C. Chottard and J. Kozelka in *Molecular Modeling of Platinum Complexes with Oligonucleotides: Methodological Lessons and Structural Insights*, (Eds.: L. Banci and P. Comba), Kluwer academic publishers, Dordrecht, **1997**, pp. 131-160.
[113] V. Murray, H. Motyka, P. R. England, G. Wickham, H. H. Lee, W. A. Denny and W. D. McFadyen, *J. Biol. Chem.* **1992**, *267*, 18805-18809.
[114] S. S. Wijmenga and B. N. M. van Buuren, *Prog. Nucl. Mag. Res. Spect.* **1998**, *32*, 287-387.
[115] H. Friebolin, *Basic One- and Two-Dimensional NMR Spectroscopy*, Wiley-VCH, Weinheim, **2004**.
[116] D. A. Case, D. A. Pearlman, J. W. Caldwell, T. E. Cheatham III, W. S. Ross, C. L. Simmerling, T. A. Darden, K. M. Merz, Jr., R. V. Stanton, A. L. Cheng, J. J. Vincent, M. Crowley, V. Tsui, R. J. Radmer, Y. Duan, J. Pitera, I. Massova, G. L. Seibel, U. C. Singh, P. K. Weiner and P. A. Kollman, *AMBER 6*, University of California, San Francisco, **1999**.
[117] T. E. Cheatham III, P. Cieplak and P. A. Kollman, *J. Biomol. Struct. Dyn.* **1999**, *16*, 845-862.
[118] M.-A. Elizondo-Riojas and J. Kozelka, *J. Mol. Biol.* **2001**, *314*, 1227-1243.
[119] Z. Chval and M. Sip, *J. Phys. Chem.* **1998**, *B 102*, 1659-1661.
[120] Z. Chval and M. Sip, *J. Mol. Struct. (Theochem)* **2000**, *532*, 59-68.
[121] M. Gellert, K. Mizuuchi, M. H. Odea and H. A. Nash, *Proc. Natl. Acad. Sci. U. S. A.* **1976**, *73*, 3872-3876.
[122] P. O. Brown and N. R. Cozzarelli, *Science* **1979**, *206*, 1081-1083.
[123] I. Turel, *Coord. Chem. Rev.* **2002**, *232*, 27-47.
[124] P. Drevensek, I. Turel and N. P. Ulrih, *J. Inorg. Biochem.* **2003**, *96*, 407-415.
[125] J. H. J. den Hartog, C. Altona, J. H. van Boom, G. A. van der Marel, C. A. G. Haasnot and J. Reedijk, *J. Am. Chem. Soc.* **1984**, *106*, 1528-1530.
[126] J. H. J. den Hartog, C. Altona, J. H. van Boom and J. Reedijk, *FEBS Lett.* **1984**, *176*, 393-397.
[127] B. van Hemelryck, E. Guittet, G. Chottard, J.-P. Girault, F. Herman, T. Huynh-Dinh, J.-Y. Lallemand, J. Igolen and J.-C. Chottard, *Biochem. Biophys. Res. Commun.* **1986**, *138*, 758-763.
[128] T. P. Kline, L. G. Marzilli, D. Live and G. Zon, *J. Am. Chem. Soc.* **1989**, *111*, 7057.

[129] K. Stehlikova, H. Kostrhunova, J. Kasparkova and V. Brabec, *Nucleic Acids Res.* **2002**, *30*, 2894-2898.
[130] O. Delalande, J. Malina, V. Brabec and J. Kozelka, *Biophys. J.* **2005**, *88*, 1-11.
[131] V. Monjardet-Bas, J.-C. Chottard and J. Kozelka, *Chem. Eur. J.* **2002**, *8*, 1144-1150.
[132] C. Giessner-Prettre and B. Pullman, *Q. Rev. Biophysics* **1987**, *20*, 113-172.
[133] F. Reeder, Z. Guo, P. d. S. Murdoch, A. Corazza, T. W. Hambley, S. J. Berners-Price, J.-C. Chottard and P. J. Sadler, *Eur. J. Biochem.* **1997**, *249*, 370-382.
[134] S. O. Ano, F. Intini, G. Natile and L. G. Marzilli, *Inorg. Chem.* **1999**, *38*, 2989-2999.
[135] Y. B. Wu, P. Pradhan, J. Havener, G. Boysen, J. A. Swenberg, S. L. Campbell and S. G. Chaney, *J. Mol. Biol.* **2004**, *341*, 1251-1269.